EXTERNAL IONIZATION SOURCE IMPROVEMENTS FOR FOURIER
TRANSFORM ION CYCLOTRON RESONANCE MASS SPECTROMETRY

By

KEITH DAVID ZIENTEK

A DISSERTATION PRESENTED TO THE GRADUATE SCHOOL
OF THE UNIVERSITY OF FLORIDA IN PARTIAL FULFILLMENT
OF THE REQUIREMENTS FOR THE DEGREE OF
DOCTOR OF PHILOSOPHY

UNIVERSITY OF FLORIDA

2004

This dissertation is dedicated to my grandfather, Rodney Lawton.

any topic that I happened to have questions about on that particular day. This dissertation would not have been possible without his guidance.

I would like to thank my family, especially my father, who has provided both encouragement and criticism at all the right times. His enthusiasm for science and learning was almost inspirational at times and was the major contribution to the genesis of my science career. My parents were the foundation of my entire academic career and I owe everything to them. I would also like to thank Ellen Stern for all of her love, devotion, and faith in me. Without her none of this would have been possible. Her support and guidance have been crucial to my success.

Finally, I would thank my late grandfather, Rodney Lawton. It was his optimism and enthusiasm that served as motivation for me during tough times. Even when I had doubts, he always believed that I would earn my doctorate. For his unwavering support, I dedicate this dissertation to my grandfather in hopes of honoring his memory.

TABLE OF CONTENTS

LIST OF TABLES

LIST OF FIGURES

Abstract of Dissertation Presented to the Graduate School
of the University of Florida in Partial Fulfillment of the
Requirements for the Degree of Doctor of Philosophy

EXTERNAL IONIZATION SOURCE IMPROVEMENTS FOR FOURIER
TRANSFORM ION
CYCLOTRON RESONANCE MASS SPECTROMETRY

By

Keith David Zientek

December 2004

Chair: John R. Eyler
Major Department: Chemistry

Fourier transform ion cyclotron resonance mass spectrometry (FTICR-MS) is

renowned for its unmatched mass resolving power and mass accuracy relative to other

conventional mass analyzers. Unfortunately, FTICR-MS suffers from limited sensitivity

for low abundance analytes. The maximum number of ions that can be trapped in the

ICR cell is determined by space charge limitations due to the finite size of the trap.

Combined with a minimum ion population requirement for detection, it is therefore

possible that low abundance ions may not be present in sufficient numbers to be detected

in the presence of more abundant species. One solution is to use an external multipole

ion guide to mass select analyte ions prior to the ICR analyzer cell. Unwanted ions are

removed prior to the cell and analyte ions are collected.

A NIST certified brass sample was analyzed on a 3T GD FTICR mass spectrometer. Modifying the applied frequency to an external octopole served to remove the low mass copper and nickel ions in the sample. After preselection, a previously undetectable signal for tin was observed. Similar experiments were performed on a commercial 4.7T ESI FTICR mass spectrometer with a contaminated sample of Angiotensin II that allowed previously undetectable charge states of angiotensin to be observed.

Atmospheric pressure photoionization is an ionization technique that offers some advantages over other conventional atmospheric ionization techniques. An APPI ionization source was constructed and interfaced to a commercial mass spectrometer for the analysis of laboratory synthesized estrogen derivatives. E1 quinol was analyzed by both APCI and APPI, proving the validity of the technique for this system.

CHAPTER 1
FTICR MASS SPECTROMETRY

Introduction

The 1989 Nobel prize winners for physics were announced in a press release dated October 12th of that year. Half the prize went to Wolfgang Paul and Hans Dehmelt, a pair of German-born physicists who had made initial studies and refinements dealing with the containment of charged particles in electric and magnetic fields. This type of instrumentation is commonly referred to as an "ion trap". It has the ability to store ions for theoretically indefinite lengths of time. Once the ions are stored, various spectrometric measurements may be performed on the ions.

Wolfgang Paul was credited with the development of the Paul Trap, which utilizes oscillatory electric fields to confine ions. Another type of ion trap, developed in the Paul lab by Hans Dehmelt, uses a combination of electric and magnetic fields and is known as a Penning trap. One of the earliest versions of the Penning trap was the Omegatron.[1] Developed in 1949 by Hipple, Thomas, and Summer at the National Bureau of Standards (NBS), the Omegatron consisted of a stacked series of square electrodes and relied upon exciting the ions until they collided with a collector plate, producing an incident current. The experiment involved the analysis of H_2^+ formed by electron ionization (EI) in a static magnetic field. A mass resolution of 35,000 was achieved in this experiment, but the researchers reported that the mass range of this instrument was limited and the mass accuracy was also limited due to space charge issues.

Due to the aforementioned limitations, ion cyclotron resonance (ICR) techniques began to take the place of the Omegatron as useful tools for mass spectrometry. ICR techniques also utilized a Penning style trap to confine ions for analysis, but relied on a dynamic magnetic field to scan through and analyze ions of different masses. Ions drifted through a region where they absorbed a radio frequency (RF) output from a irradiating oscillator. The ions absorbed the energy through a process to be described later, and the change in power was measured by the resonant circuit of a marginal oscillator detector. As the magnetic field was scanned, different ions came into resonance. While the ICR mass spectrometer demonstrated significant advantages in mass resolution and trapping efficiency, it suffered from several limitations.[2-4]

The first of these involved the restriction of using a swept magnetic field. It would often take 10 to 15 minutes to perform a single scan using the variable field electromagnets. It was necessary to perform a scan for even longer times to achieve the highest resolution possible for the technique.

The second limitation stemmed from the initial cell designs, which were often segmented and required the ions to drift through the analyzer region. In this setup ions are detected only once and could not be trapped for long times, placing limitations on reaction and kinetics experiments. Current analyzer cells do not suffer from this limitation due to advances in their design.

The third limitation stemmed from the physical size and field strength constraints inherent to using a electromagnet to produce the magnetic field. At the time, the only swept-field magnets were electromagnets with limited upper limits in field strength, so the mass range was limited to several hundred amu. The relatively small distance between the magnet pole faces also prevented the use of large analyzer regions due to

size constraints. While the development of superconducting magnets with larger

magnetic fields and increased diameter bores could help to alleviate these problems, it

was the introduction of Fourier transform techniques that would revolutionize mass

spectrometry.

In 1974, Comisarow and Marshall first successfully applied the Fourier transform

technique to ICR creating the first Fourier transform ion cyclotron resonance (FTICR)

mass spectrometer.[5] The following section will overview some of the concepts essential

to understanding FTICR mass spectrometry.

Ion Motion in a Magnetic Field

Like the original ICR, the FTICR mass spectrometer relies upon magnetic and

electric fields to confine ions for analysis. If we introduce an ion into a homogeneous

magnetic field, the ion is subjected to a Lorentz force as defined by:

$$F = q(v \times B_0) \tag{1.1}$$

where m is the mass of the ion, q is the charge of the ion, v is the velocity of the ion, and

B_0 is the magnetic field strength.

It is known that:

$$F = ma \tag{1.2}$$

$$F = m d \frac{v}{dt} \tag{1.3}$$

Equation 1.1 indicates that the ions will be subjected to a force perpendicular to the

magnetic field. This force causes the ion or group of ions to be bent into a circular path

along a plane perpendicular to the magnetic field lines. Positive ions will move counter-

clockwise to the direction of the magnetic field.
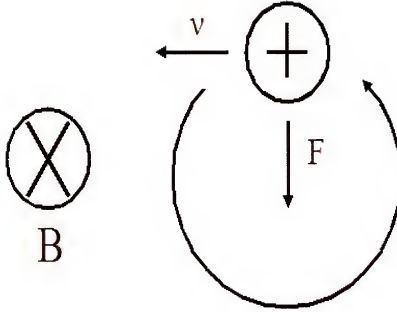
Figure 1.1. The Lorentz force acts upon charged particles in the presence of an external magnetic field, B_0.

Since $\dfrac{dv}{dt} = \dfrac{v_{xy}^2}{r}$ for an object with uniform circular motion, we can substitute

this equation into equation 1.1 and 1.3 to obtain

$$F = \frac{m v_{xy}^2}{r} \tag{1.4}$$

And

$$F = q v_{xy} B_0 \tag{1.5}$$

Both can be combined to produce

$$\frac{m v_{xy}^2}{r} = q v_{xy} \boldsymbol{B_0} \tag{1.6}$$

If we substitute in the angular velocity, defined as $\omega = \dfrac{v_{xy}}{r}$, equation 1.6 becomes:

$$F = m\omega^2 r = q\,\omega\,r\,\boldsymbol{B_0} \tag{1.7}$$

Cancellation of terms and rearrangement for ω gives the cyclotron frequency:

$$\omega_c = \frac{qB_0}{m} \tag{1.8}$$

This equation gives the angular frequency of the ion in the presence of an external

magnetic field, B_0. Knowing that $\upsilon = \dfrac{\omega}{2\pi}$, we can divide equation 1.8 by 2π to produce

$$\upsilon_c = \frac{qB_0}{2\pi m} \tag{1.9}$$

This linear frequency expression allows us to calculate the so-called "ICR orbital frequency." Equation 1.8 is commonly called the cyclotron equation, denoting the frequency at which the ions will move in a circular path due to the Lorentz force.

From equation 1.8, we can deduce several assumptions about the behavior of ions in a magnetic field. Most importantly, the kinetic energy of the ions does not appear in the equation. This means that a homogeneous group of ions can have wide distribution of kinetic energies, but the cyclotron frequency of the ions will remain constant. While the discussion has been focused on radial confinement of the ions along the x and y axis due to an external magnetic field, nothing has been said about confining the ions along the z axis, located parallel to the magnetic field. Ions are free to move axially along the magnetic field lines and might be lost from the trapping region.

Ion Trapping

Trapping the ions for extended time periods requires the application of a small voltage to either end of the trapping region, commonly known as the "cell."
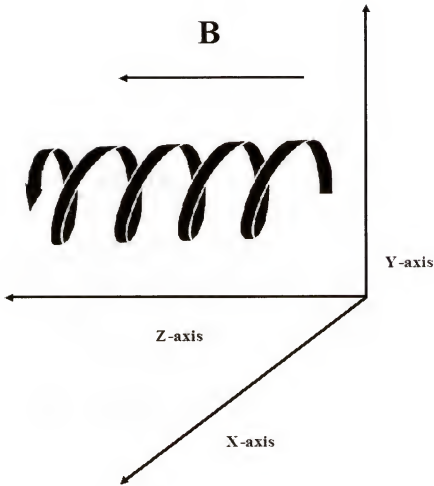
Figure 1.2. Ion motion which is radially confined in the x and y directions by an externally magnetic field, B, acting along the z axis.

This is usually accomplished by placing two electrodes at either end of trapping region perpendicular to the magnetic field. A voltage is applied to each of them which has the same polarity as the ions to be trapped. This creates a potential well inside the magnetic field, trapping the ions along the z axis. The ions are then trapped near the center of the cell and oscillate back and forth between the two axially positioned trapping electrodes.
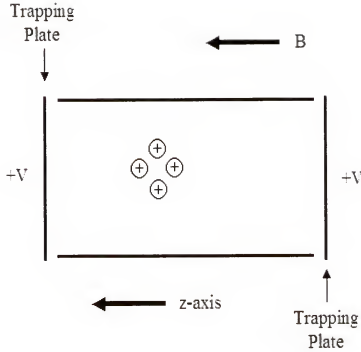
Figure 1.3. A positive voltage applied to the trapping plates will confine ions axially in the ICR analyzer cell.

Ions trapped in this way will have a characteristic sinusoidal oscillation frequency given by the following equation

$$\omega_z = \sqrt{\frac{2qV_T\alpha}{ma^2}} \tag{1.10}$$

where α is a constant determined by the geometry of the trapping cell, a is the distance between the two trapping electrodes, and V_T is the potential applied to the trapping electrodes.[6]

Due to the aforementioned physical limitations of the superconducting magnets commonly used in this technique, it is unlikely that a set of trapping plates will be infinite area. Therefore, the trapping potential is not constant throughout the cell. This leads to an equation describing the radial force acting upon the ions due to the trapping potential.[6]

$$F_{radial} = m \omega r^2 = \frac{q V_T r \alpha}{a^2} \tag{1.11}$$

At the center of the cell and along the z-axis, the potential is at a maximum. Moving outward, the potential decreases along the x and y axis. This potential gradient pushes the ions radially outwards, in opposition to the Lorentz force pushing inwards. It is possible to write an equation describing the force acting on an ion in the presence of a static magnetic field and an axial voltage,

$$F = q B_0 \omega r - \frac{q V_T r \alpha}{a^2} \tag{1.12}$$

which can be rewritten as

$$\omega^2 - q B_0 \frac{\omega}{m} + q V t \frac{\alpha}{m a^2} = 0 \tag{1.13}$$

By solving for ω, it is possible to obtain a new expression for the cyclotron motion of an ion in the presence of a static magnetic field and an axial voltage in a cell of finite size. Since equation 1.13 has the form "$ax^2 + bx + c = 0$," the quadratic equation can be used to obtain the two roots equal to ω.

The first root describes the slightly modified cyclotron frequency

$$\omega_+ = \frac{\omega_c}{2} + \sqrt{\left(\frac{\omega_c}{2}\right)^2 - \frac{\omega_c^2}{2}} \tag{1.14}$$

The second root describes a new type of motion know as the magnetron motion

$$\omega_- = \frac{\omega_c}{2} - \sqrt{\left(\frac{\omega_c}{2}\right)^2 - \frac{\omega_c^2}{2}} \tag{1.15}$$

It is important to note that the magnetron frequency is less than the cyclotron frequency. Therefore, it is possible to excite the ions by bombarding them with energy in the rf region of the electromagnetic spectrum corresponding to the cyclotron frequency.

Excitation (Single Frequency)

Unfortunately, there is little analytical utility in the normal cyclotron motion of ions. However, we can devise a situation where the ions rotating in a static magnetic field are exposed to an oscillating electric field component of an applied electromagnetic field. If the field is oscillating at a frequency close to the cyclotron frequency, the ions will absorb the energy from the field and be pushed forward in their trajectories. This serves to increase the radius of the ions in the analyzer cell.

For the majority of ions of interest, the cyclotron frequency is approximately 0.5 to 3 MHz, corresponding to the radio frequency (rf) region of the electromagnetic spectrum. Two "excitation" electrodes, located parallel to the magnetic field, are used to increase the ion's radius. Figure 1.4 shows the effects of an applied rf voltage on a initially incoherent group of ions.

The radius of the ions after excitation can be calculated using the following equation:[6]

$$r_{excite} = \frac{V_{p-p}T_{excite}}{2dB_0} \tag{1.16}$$

where V_{p-p} is the peak to peak amplitude of the applied rf, T_{excite} is the period of time in which the rf voltage frequency is in resonance with the ion's frequency, d is the distance separating the two excitation electrodes, and r_{excite} is the radius of the ions after excitation. It is also important to note that the cyclotron radius is not dependent on either mass or charge. Therefore, ions of a variety of m/q values can all be excited to the same radius.

When ions are introduced into the cell, the phase of the orbital motion is random. A situation can be posited where two ions are 180^0 out of phase with each other. As one ion draws close to an electrode, the other ion is nearing the opposite electrode.
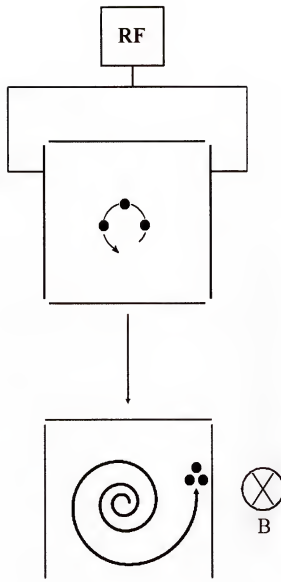
Figure 1.4. Ions are initially confined near the center of the cell in a partially incoherent packet. Upon the application of an rf pulse to the excitation electrodes, the ions are accelerated to a coherent packet in a larger orbit.

This would serve to cancel out the charges and produce no net current between the electrodes used for detection. An important advantage of resonant excitation is that a spatially coherent packet of ions is created from an initially incoherent clump of ions.

Detection (Single Frequency)

The normal cyclotron radius for a typical group of ions at room temperature is too small for any type of detection. Since an applied rf pulse can be used to increase the radius of the ions in the cell, it is possible to impart enough energy into the ions that they will collide with the cell walls. This procedure of excitation to collision was the basis of detection for the classical Omegatron technique discussed earlier in this chapter.

In the FTICR method, ions are excited just enough to increase their radius to a point where they are in close proximity to the walls of the analyzer cell. Another pair of electrodes are positioned at right angles to the excitation electrodes. This second set of electrodes are commonly known as the "detection" electrodes. As the excited cluster of ions draws close to each of the detection electrodes, it either attracts or repels electrons in the electrodes. If the two electrodes are connected as part of an electric circuit the oscillating clump of ions creates a differential current between the electrodes that has the same characteristic frequency as the cyclotron frequency of the ions. Figure 1.5 shows the motion of a clump of positively charged ions in the analyzer cell.

The magnitude of this differential current is given by the difference in charge induced between two infinite electrodes according to the equation:

$$\Delta Q = \frac{-2qy}{d} \tag{1.17}$$

where ΔQ is the charge difference, q is the charge of the ion, d is the distance separating the two detection electrodes, and y is the location of the ion on a plane perpendicular to the electrodes. From this equation it can be deduced that the detected current is proportional to the charge, but also directly proportional to the excitation radius (y). Normal detection modes convert this current to a voltage signal by means of an
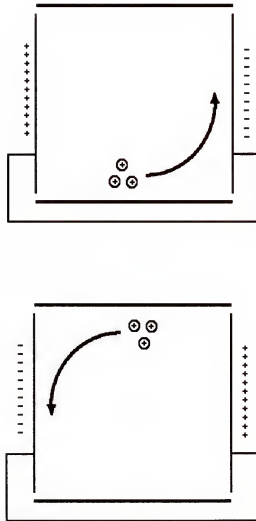
Figure 1.5. The movement of the excited ion adjacent to the detect plates induces a sinusoidal current in the plates. The frequency of the current is equivalent to the cyclotron frequencies of the ions.

operational amplifier current-to-voltage converter. Figure 1.6 shows how the induced current is measured over time. In the presence of collisions with background neutrals or other ions, the excited ion will not remain at the excitation radius. The ions will relax down to their initial radius near the center of the cell, producing an induced current that decreases over time.

Time
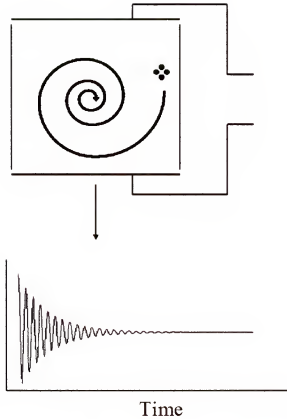
Figure 1.6. As the radius of the ions decreases due to collisions between background neutrals and other molecules, the induced signal also decreases.

Since the induced current is proportional to the number of ions in the cell, it is possible to calculate the minimum number of ions needed for detection of a voltage signal. The following equation gives the voltage signal for a single ion[7]

$$V(t) = (\frac{q}{2C}) A_1(r) \cos(\omega_+ t) \tag{1.18}$$

where C is the capacitance between the two electrically connected detection electrodes and $A_1(r)$ is a coefficient proportionally related to r which can be determined mathematically.

The voltage for a group of N ions is equal to

$$V(t) = (\frac{Nq}{2C}) A_1(r) \cos(\omega_+ t) \qquad (1.19)$$

Solving for N gives

$$N = \frac{2CV(t)}{q A_1(r) \cos(\omega_+ t)} \qquad (1.20)$$

or

$$N = \frac{2CV_{p-p}}{2q A_1(r)} \qquad (1.21)$$

$$N = \frac{CV_{p-p}}{q A_1(r)} \qquad (1.22)$$

By substituting typical values for the parameters in the above equation it is possible to determine the minimum number of ions needed for a signal to noise ratio of 3:1. Numbers obtained both experimentally and theoretically indicate that a value of ~200 ions is needed for detection.[7] This indicates that there is a possibility for a scenario where ions can be in the cell, but are not present in sufficient quantities to allow for detection.

Fourier Transform

Once the voltage signal has been produced by the operational amplifier, the resultant signal is amplified and digitized by an analog to digital converter (ADC) circuit. The digitized signal is composed of a sinusoidal frequency corresponding to the m/q of the ions in the analyzer cell. While this sinusoidal component contains information about the m/q, it is necessary to manipulate the data into a more user-friendly format. This is accomplished by using the Fourier transform.

This mathematical method allows a single frequency or group of frequencies in a

time domain spectrum to be converted into a frequency domain spectrum where the frequencies are represented by peaks in the spectrum. By deriving a simple calibration formula from the cyclotron equation, it is possible to easily convert the frequency domain data into a more familiar mass spectrum. Figure 1.7 shows the conversion of a time domain voltage into a frequency domain spectrum by Fourier transformation and mass calibration.
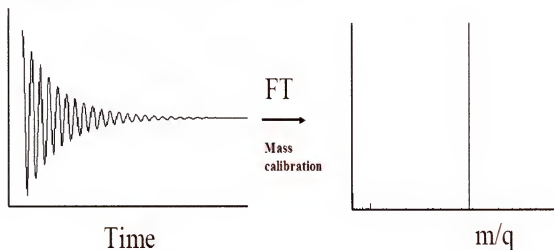
Figure 1.7. The mathematical Fourier transform converts a time domain signal into a frequency domain spectrum. Mass calibration gives the m/q mass spectrum.

Fourier transform methods all give a frequency domain spectrum that is equivalent to the same spectrum obtained by sweeping infinitely slowly across a variety of m/q values. There is also the multiplex, or Fellget's advantage, where the signal to noise ratio (S/N) of N spectra can be increased by $\sqrt{N}$. The capacity for fast measurements and signal averaging makes Fourier transform ICR extremely powerful relative to conventional ICR.

Excitation (Broadband)

Previously, only the simplest case of single m/q ions was considered in this

treatment. Fourier transform methods allow for simultaneous detection of a large number of ions with different m/q. While the speed of detection can be greatly increased by using Fourier transform methods, it is important to note that the length of time at which the transient response is measured is directly related to the resolution achievable by

$$R = \frac{f_c t}{2} \qquad (1.23)$$

where R is the maximum theoretical resolution, f_c is the cyclotron frequency, and t is the time duration of the transient. This would imply that to increase the resolution of FTICR, one would simply need to sample for longer periods of time.

However, the transient lifetime is limited by two major factors. The first is that a perfect vacuum cannot be maintained in the analyzer cell and the excited radius is pressure-limited by collisions with background neutrals and other ions. This creates a transient that decays over time similar to what is seen in NMR spectroscopy shown schematically in figures 1.6 and 1.7. Maintaining ultra-high vacuum in the analyzer cell is essential for obtaining high resolution spectra.

Another major limitation is the available memory in the ADC for digitization. The Nyquist criterion states that the sampling rate must be at least twice the highest frequency being sampled to avoid aliasing effects. It seems logical that increasing the sampling rate would prevent such effects. However, the sampling rate is inversely proportional to the time duration of the transient given by the following equation

$$T = \frac{N}{S} \qquad (1.23)$$

where N is the number of data points in the spectrum and S is the sampling rate of the ADC digitizer.

These limitations must be taken into consideration when performing broadband

detection with FTICR mass spectrometry. Each of the above serves to limit the ultimate resolution available. Luckily, there are other techniques that can be used to increase the resolution of a broadband spectrum, most notably by varying the magnetic field strength.

FTICR Compared to Other Mass Analyzers

Due to the cost of purchasing and maintaining a high field magnet, FTICR mass spectrometers are the most expensive commercially available mass analyzers. But the high cost is balanced by a variety of advantages that make FTICR quite appealing for experimental work.

FTICR mass spectrometry measures the frequency of the induced current of a group of ions and not the current produced by destructive neutralization with a detector as used by other types of mass analyzers. Due to advances in electronics over the last fifty years, it is now possible to measure frequency very precisely and very accurately. This gives FTICR the highest resolution of any mass analyzer by an order of magnitude with no loss in sensitivity. The mass accuracy is also incredibly high, approaching the ppb level.

With the exception of the newly developed Orbitrap,[8] no other mass analyzer can non-destructively measure the m/q of ions on a regular basis. This allows for theoretically infinite trapping and the remeasurement of a single population of ions. Ions can also be isolated for reaction with other chemicals or photons, and the resultant products can be measured. The ultra-high vacuum in the analyzer cell allows for minor interactions between ions and background gases, making FTICR an effective platform for ion-molecule reaction studies.

Advantages of Increased Magnetic Field Strength

The cyclotron frequency of trapped ions is directly proportional to the magnetic field strength as described in equation 1.8.

By taking the first derivative of the cyclotron equation with respect to m

$$\frac{d\omega_c}{dm} = -\frac{qB_0}{m^2} \tag{1.24}$$

which simplifies to

$$\frac{m}{\Delta m} = \frac{qB_0}{m\,\Delta\omega_c} \tag{1.25}$$

where Δm is the mass calibrated frequency domain spectral peak width at some predetermined fraction (usually 50% of the peak maximum height).

Thus, this equation states that peak resolution is directly proportional to the magnetic field strength. Several other important features can be determined by manipulating the cyclotron equations, and all relate to magnetic field strength. Resolution, axialization efficiency, and scanning speed all increase linearly with magnetic field strength. The upper mass limit, ion trapping time, ion energy, and maximum number of ions able to be stored all increase quadratically with magnetic field strength.

Broadband Excitation Schemes

One of the most prominent advantages of using Fourier Transform for detection is the ability to simultaneously collect information for a large number of ions. Several types of broadband excitation are utilized in FTICR mass spectrometry. These include single frequency shots, chirp excitation, and stored waveform inverse Fourier transform (SWIFT)[9] excitation.

A single frequency shot has been previously described in the section detailing

single frequency excitation events. Simply, it is the application of a single rf frequency for a predetermined time. The duration of the excitation is important, because too long an excitation pulse will push the excited ion to the walls of the cell, where it will either be neutralized by collision with the walls.

During a chirp excitation event, also known as a frequency sweep excitation, all ions over a previously determined m/q range are excited virtually simultaneously. This is achieved by scanning through the range of excitation frequencies at a fast rate. A solution to this problem lies in the SWIFT waveform.[9] Creating a SWIFT waveform starts by designing the desired frequency range for excitation and then using a Fourier transform to convert it to the time domain. This results in a smoother power distribution for the excitation event as well as allowing for the placement of notches into the excitation profile. This is by far the most useful and versatile of all the above techniques, allowing for a wide variety of excitation-ejection waveforms that have very uniform power profiles.

It is important to note that all of the aforementioned excitation techniques can be used to eject ions from the cell. In the situation where there are two groups of ions, one in high abundance and one in low abundance, the signal from the high abundance ions will have a tendency to overwhelm the signal from the low abundance ions. Isolation of ions can also have experimental utility by removing background and fragmentation ions before reaction of desired ions with any number of species. While this can be useful it should be mentioned that ejection schemes do not increase the total number of ions in the cell; their only purpose is to remove ions by ejection. If an ion is present in insufficient quantities for detection, isolation will not aid in detection.

FTICR Pulse Sequences

Since the detection electrodes in FTICR are simply a set of sensitive radio antenna, an rf excitation pulse will drown out any available signal generated by cyclotron motion of ions. This is circumvented in other mass analyzers by spatially separating the different regions, but this is impossible in FTICR mass spectrometry. Mass analysis and detection take place in the same physical space, so it becomes necessary to separate these events temporally.

A typical sequence of events includes ionization/injection, excitation, and detection events. More complicated pulse sequences can be created and combined with complicated excitation sequences described earlier to isolate single ions or groups of ions from a complex initial sampling of ions.

Components of an FTICR Mass Spectrometer

Every FTICR mass spectrometer consists of five major components. The first of these is the magnet, an essential component of the Penning trap necessary for creating the magnetic field for radial trapping. Magnets can be either permanent, electromagnetic, or superconducting. The last has become the most commonplace due to superior field homogeneity and high field strengths. This is an important consideration due to the various advantages conferred by larger magnetic fields. Most superconducting magnets sold range from 3 to 9 T, with 7T becoming the most common sold at the current time. Higher field strengths have been tested at the National High Magnetic Field Laboratory (NHMFL) in Tallahassee, most notably using a 25T resistive magnet.[10]

The second component of an FTICR mass spectrometer is the vacuum system. Collisions with background neutrals at atmospheric pressure or high vacuum (10^{-3} to 10^{-5}

torr) would prevent ion trapping in any fashion. Even at the upper limits of very high vacuum (10^{-6} to 10^{-8} torr), collisional damping would serve to increase the decay time and thereby inhibit resolution. Typically, an FTICR mass spectrometer operates in the ultra-high vacuum regime (10^{-9} torr and lower) to achieve maximum performance. The types of pumps as well as the size of the pumps depend on the experiment at hand, as different pumping speeds may be needed for different experiments.

The third component is the FTICR analyzer cell. This consists of at least six electrodes: two for excitation, two for detection, and two for axial trapping. Early experiments arranged six platelike electrodes in a cubic configuration to create an analyzer cell. Due to the cylindrical bore of most superconducting magnets, excitation and detection electrodes with a circular curvature matching the inside of the vacuum can have become popular in recent years due to increased internal capacity. A variety of other cell geometries have been explored over the years, but none have become commonplace.[11]

As discussed previously, FTICR mass spectrometry measures the m/q values for *ions* in the *gas* phase. It is therefore necessary to ionize the molecules in the sample of interest as well as somehow transfer it to the gas phase. Depending on the application, there are a variety of ionization sources available to mass spectrometry. Electron ionization,[5] matrix assisted laser desorption (MALDI),[12] and electrospray ionization (ESI)[13] are all common ionization techniques that have been used with FTICR mass spectrometry. The research referred to in this thesis used ESI and glow discharge (GD) ionization to produce ions. Each ionization method will be discussed further in their respective sections.

Early ICR and FTICR mass spectrometers relied on internal ionization sources located adjacent to or inside the analyzer cell. With the advent and increasing popularity of atmospheric pressure ionization techniques, most instruments now come equipped with ion optics and multiple stages of differential pumping to handle external ionization sources. Examples of ion optics used for transfer include electrostatic ion optics,[14] rf ion optics,[15] and multipole ion guides.[16] The latter is an important technique and its versatility and use will be discussed further in Chapter 2. Figure 1.8 shows a typical FTICR mass spectrometer outfitted with an Electron Ionization (EI) source.
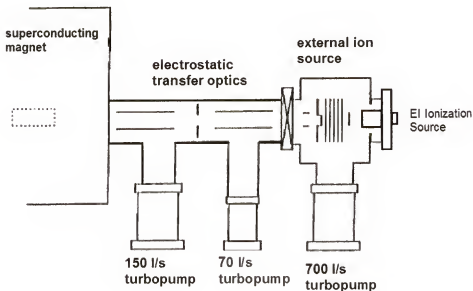
Figure 1.8. A typical FTICR mass spectrometer outfitted with an Electron Ionization (EI) source.

The fifth component of an FTICR mass spectrometer is the associated electronics and software. Every FTICR system has to include three important electrical components necessary to obtain spectra. Initially, a *arbitrary waveform generator* is

necessary for the construction and creation of the rf waveform needed for excitation. Once the ions are excited, some type of *pre-amplifier* is needed to amplify the signals for processing. The final piece is an ADC to convert the analog voltage signal to a digital signal that can be sampled by the *digitizer* for analysis. While the software differs greatly from system to system, every instrument contains some version of these three pieces of electronic. The final component of the FTICR mass spectrometer is a computer and software used to operate the mass spectrometer. The computer is used to provide an platform for which to run the software necessary to control the electronics described in the previous paragraph. The computer is also used to run any software designed to allow user control of operational and data acquisition parameters. Most software packages also come with some type of data analysis software to allow user manipulation of the acquired data.

Conclusions

The intent of this section was to provide a theoretical background for some of the fundamentals of FTICR mass spectrometry. The high mass resolving power and mass accuracy have made FTICR mass spectrometry a very desirable technique for a wide variety of analytical applications. These fundamentals will be discussed in further chapters as they relate to improving sensitivity for low abundance ions.

Chapter 2 will cover some of the fundamental theory behind the operation of multipole ion guides and how they relate to ion transfer. All multipoles can act as a low resolution mass filters allowing for the removal of unwanted background ions. Chapter 3 will focus on using the aforementioned preselection techniques to improve the selectivity of detection for high mass, low abundance ions created by glow discharge (GD)

ionization. Chapter 4 will discuss experiments with electrospray ionization and some explorations of preselection using a commercial hexapole ion guide. Chapter 5 will cover the analysis of biologically important estrogen derivatives with a laboratory-built atmospheric pressure photoionization source.

CHAPTER 2
MASS SELECTION IN MULTIPOLE ION GUIDES

Introduction

J.J. Thomson's determination of the mass-to-charge ratio of the particles found in a cathode ray was the first mass measurement of a gas-phase ionic species.[17] His initial studies and subsequent experiments in X-ray scattering cross sections were the beginning of research into the interactions of charged particles in the presence of electromagnetic fields.

Over the last century, mass spectrometry began to see use by organic chemists as a potential tool for organic structure elucidation. Early mass analyzers were very limited in both resolution and mass accuracy, which was only of minor concern to organic chemists. As scientists began to see the utility of the mass spectrometric technique, mass analyzers and ion optics began to grow in complexity.

In recent years, three-dimensional time-varying multipolar potentials have found increased usage for transportation and measurement of ionic species. An electric field is generated by applying a radio frequency (rf) potential to a series of metal rods aligned parallel to each other with cylindrical symmetry.

Theoretically the rods should have a hyperbolic cross-section for optimal performance, although rods with a cylindrical cross section have been deemed sufficient and are significantly less difficult to machine. Studies have shown that a series of rods with a radius (r) arranged cylindrically around an inscribed radius (r_0) can best approximate a hyperbolic field if the relationship is $r = 1.148 r_0$.[18]

To further elucidate the behavior of charged particles in the presence of multipolar potentials, consider the case of a time-dependent voltage applied to two rods equidistant from a central, longitudinal axis and positioned on opposite sides of the central axis.

Assume for this case that a group of positively charged ions is introduced between the two rods. If a sinusoidal potential with an average value of 0 volts is applied differentially across the two rods, during a full cycle of the applied rf, one rod will spend one-half of that cycle at a positive potential and the other rod will spend one-half at a negative potential during the same half cycle due to the sinusoidal shape of the waveform applied to the rods. Figure 2.3 shows the behavior of a positive ion in between two rods while an rf voltage is differentially applied to each rod.
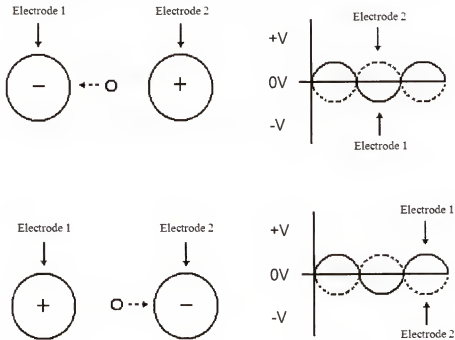
Figure 2.1. Behavior of a positive ion centered between two electrodes. A sinusoidal waveform is applied to electrodes 1 and 2. The waveform applied to electrode 2 is 180 degrees out of phase from the waveform applied to electrode 1.

Therefore, the net potential along the central axis will be zero. Positively charged ions introduced into the system will be accelerated towards a rod during negative potential half-cycles and accelerated away from a rod during the positive potential half-cycles. If the frequency is sufficiently high, the potentials will change fast enough that the ions will stay close to the central axis. During the negative potential half-cycle, the ions will be focused toward the rods and away from the central axis. The overall effect will be that the ions oscillate back and forth around the central axis due to the potential field created by the applied sinusoidal waveform.

A very light ion may achieve sufficient acceleration during the negative potential half-cycle that it will collide with a rod. This will cause the ion to become neutralized and therefore to be exempted from our consideration. A heavy ion will respond very slowly to the changes in the electric field. To eject a heavier ion, the frequency would have to be decreased to a point where all of the lighter ions have already collided with the rods and been neutralized. It should be apparent for a system of two sets of two rods with a differentially applied rf that the rods can act as a high-pass mass filter by merely decreasing the applied frequency to a value where lighter ions are lost by collision with the rods.

Now consider the addition of a constant (DC) voltage bias to the applied rf voltage. The average potential applied to the rods will be dominated by the DC voltage if the amplitude of the voltage is sufficiently large. Both light and heavy ions will feel the influence of only the effective DC potential and their motion will be heavily influenced by the polarity of the DC voltage. If the applied potential is large and positive, all positive ions will be focused toward the central axis and towards the spacing in between adjacent rods. In this case, ions will be lost from the system due to ejection. If the

applied potential is large and negative, then the effective average applied potential will be negative and all ions will be drawn toward the rods, where they will collide and be neutralized.

At low values of the applied DC voltage, heavier ions will still feel the effect of the average applied potential, but lighter ions will be influenced more by the fluctuating rf potentials. The heavier ions will thereby be either ejected or neutralized while lighter mass ions will remain confined between the two rods. Therefore, an applied DC voltage can act as a low-pass mass filter.

Now consider the case of four rods arranged with cylindrical symmetry around a central axis (z) and positioned equidistant from the z-axis along the x and y axes. This arrangement is commonly referred to as a quadrupole. One set of two rods will lie on the x axis and another set of two rods will lie on the y axis so that each rod is parallel and radially arranged around the central axis, as shown in figure 2.1.
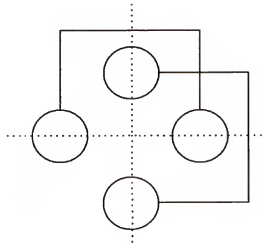
Figure 2.2. Cross-sectional view of a quadrupolar arrangement of electrodes. Not to scale.

A unique situation will be achieved if a sinusoidal waveform is applied to one set of rods while the same waveform is applied to the other set of rods 180 degrees out of phase. If the applied waveform has a frequency in the low (LF) to high (HF) frequency range of the rf spectrum, (30 kHz to 30 MHz) then the rapidly oscillating potentials prevent ions from being attracted preferentially to one set of rods.
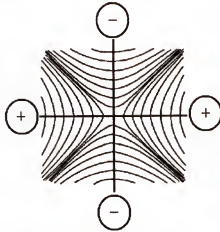
Figure 2.3. Equipotential lines in a quadrupolar arrangement of electrodes. Expanded to show detail.

This creates what could be considered to be a field-free region lying along the central axis between the rods. By choosing the correct frequency and amplitude parameters for the applied rf voltage, stable conditions can be produced inside the quadrupole, allowing for the transport of ions accelerated along the central, z-axis. The response of ions to frequency and rf amplitude is similar to that experienced in the dipolar arrangement mentioned previously. Up to this point, a quadrupole operating only with an applied rf potential has been discussed. Now, consider the application of a DC voltage bias applied along with the rf to the rods. If a sufficiently positive voltage is applied to one set of the rods, then heavier ions will be repelled toward the other set of rods and be neutralized. It is then possible to operate the quadrupole as a low-pass mass filter by applying a large DC voltage bias to the rods.

The combination of DC and rf voltages can then be manipulated to allow ions of a specific m/q to pass through the quadrupole instrument. Ions with a higher or lower m/q than the mass of interest can be removed by increasing the DC bias on the rods, while ions of a smaller m/q than the mass of interest can be removed by manipulating the applied rf and DC parameters. The quadrupole ion guide can thus be used as a mass filter, selectively allowing only specific ions to pass through. Fortunately, it is relatively easy to model the equations of motion for an ion in a quadrupolar field.

Equations of Motion in a Quadrupole

If the central axis of a quadrupole is defined as the z-axis, it is possible to calculate the potential surface distribution inside the quadrupole at any time(t).[19]

$$\Phi = [U + V cos(\omega t)] \frac{x^2 + y^2}{2 r_0^{\,2}} \tag{2.1}$$

where r_0 is the inscribed radius from the z-axis to the surface of an electrode, V is the amplitude of the rf potential, U is the DC offset of the applied rf potential, ω is the angular frequency of the applied rf, r_0 is the inscribed radius of the quadrupole, and x and y are ion's distance from the respective axis.

Obviously, the applied potentials at each electrode will determine the resultant potential distribution. By taking the partial derivative of equation 2.1 with respect to each axis we can determine the electric field along each axis

$$E_x = \frac{-d\Phi}{dx} = -[U + V cos(\omega t)] \frac{x}{r_0^{\,2}} \tag{2.2}$$

$$E_y = \frac{-d\Phi}{dy} = -[U + V cos(\omega t)] \frac{y}{r_0^{\,2}} \tag{2.3}$$

$$E_z = \frac{-d\,\Phi}{dz} = 0 \tag{2.4}$$

Since we know that $\mathbf{F} = q\mathbf{E}$, it is then possible to calculate the force on a charged particle along each axis from the above equations.

$$F_x = -[U + V cos(\omega t)]\frac{qx}{r_0^2} \tag{2.5}$$

$$F_y = -[U + V cos(\omega t)]\frac{qy}{m r_0^2} \tag{2.6}$$

$$F_z = 0 \tag{2.7}$$

The quadrupole ion guide acts similar to a Penning trap as described in chapter 1 since it is possible to infer from the above equations that an applied potential will no affect the motion of a charged particle along the z-axis.

Using $F = ma$, $a = \frac{d\,v}{dt} = \frac{F}{m}$

$$\frac{d^2 x}{dt^2} - \frac{qx}{m r_0^2}[U + V cos(\omega t)] = 0 \tag{2.8}$$

$$\frac{d^2 y}{dt^2} - \frac{qy}{m r_0^2}[U + V cos(\omega t)] = 0 \tag{2.9}$$

$$\frac{d^2 z}{dt^2} = 0 \tag{2.10}$$

The above equations can be used to calculate the trajectory of any ion as long as its initial position is known. It should be noted that the above equations assume that the electrodes have a hyperbolic cross-section for purposes of simplification. Two new quantities, designated by a_n and q_n where n is the order of the multipole, can be defined.

$$a_2 = \frac{4qU}{\omega^2 r_0^2 m} \tag{2.11}$$

$$q_2 = \frac{4qV}{\omega^2 r_0^2 m} \tag{2.12}$$

These represent the so-called "stability equations" for a quadrupole mass filter.

Equations 8 and 9 can now be rewritten to state

$$\frac{d^2 x}{dt^2} + \frac{\omega^2}{4}[a_2 + 2q_2 \cos(\omega t)]x = 0 \tag{2.13}$$

$$\frac{d^2 y}{dt^2} + \frac{\omega^2}{4}[a_2 + 2q_2 \cos(\omega t)]y = 0 \tag{2.14}$$

These can be then changed into a "canonical" form of the well-studied Mathieu equations[19]

$$\frac{d^2 u}{d\xi^2} + [a_u + 2q_u \cos(\omega t)]x = 0 \tag{2.15}$$

where $\xi = \frac{t}{2}$ and u is a parameter that can represent any of the axial coordinates, such as x or y.

Emile Léonard Mathieu was a French mathematician born in 1835, who developed a series of solutions to equations of the type given in equation 2.15 above, known as the Mathieu functions.[20-22] The solutions were divided up into categories of bounded and unbounded solutions. Applied to the case of a quadrupole mass filter, the bounded solutions represent a case where the location of a charged particle remains finite along the x and y axes. Physically, this corresponds to a stable trajectory along the z-axis. Conversely, an unbounded solution represents the case where the charged particle would move without limits in the x and y directions. This represents an unstable trajectory, such

as collision with the electrodes or ejection from the quadrupole ion guide. Some sample trajectories are shown in figure 2.4.
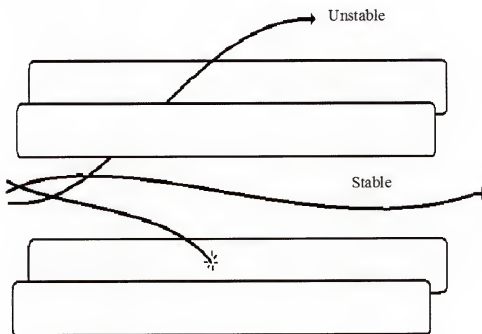
Figure 2.4. Stable and unstable ion trajectories in a quadrupole ion guide.

Further examination of the stability equations leads to the conclusion that stability depends on the a_2 and q_2 parameters. This allows one to plot a graph of a_2 vs. q_2 depicting the regions where solutions to the equations are either stable or unstable.

Figure 2.5 shows the a_2-q_2 stability diagram. The above treatment simplifies the stability concept by reducing it from a problem involving many variables (V, U, ω, q, m, r_0) to a problem involving only a_2 and q_2. Upon examination, it becomes apparent that the stability diagram can be used to plan schemes for mass selection. In fact, this diagram
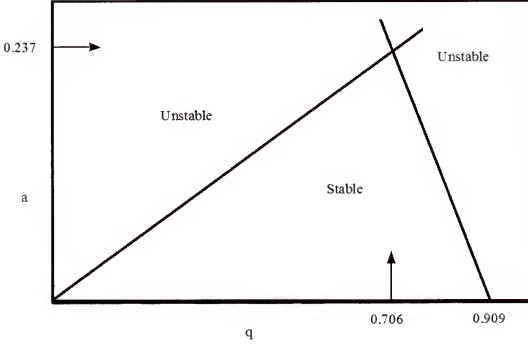
Figure 2.5. Theoretical stability diagram for a quadrupole ion guide.

can be used to confirm the general comments made about mass selection in the previous section. Keeping all other parameters constant, it is clear that manipulating U(DC) and V (rf) can be used to manipulate the a_2 and q_2 values for an ion. This theory can now be extended to higher order multipoles such as hexapoles and octopoles.

It is possible to derive general equations for many values of n for a_n and q_n[23]

$$a_n = \frac{n^3 q U}{2 \omega^2 r_0^2 m} \tag{2.16}$$

$$q_n = \frac{n^3 q V}{4 \omega^2 r_0^2 m} \tag{2.17}$$

Substituting the order of a quadrupole (2) for n into the equations produces equations 11 and 12.

Stability Diagrams for Multipoles

Szabo and Hägg have produced a series of papers that simulated ion motion for quadrupoles, hexapoles, and octopoles using the general stability equations described above.[23] They performed computer simulations of ion motion using the equations and described simulated ion stability diagrams for quadrupoles, hexapoles, and octopoles. The general theory described above is taken from this series of papers.

Using the general equations for a_n and q_n, Szabo performed a series of computer simulations of the trajectories of ions for multipoles of order n=2, n=3, and n=4. By examining the output and the results of trajectory simulations, the authors were able to determine crude stability diagrams for each of the aforementioned values of n. This corresponds to the stability diagrams for a quadrupole, hexapole, and an octopole.

Figure 2.6 depicts the test calculation for a quadrupole ion guide (n=2). When compared to the theoretical stability diagram in figure 2.6, it is apparent that the test calculation closely mirrors the theoretical dimensions and shape of the stability diagram for stable motion. Note that the a_2 and q_2 maxima in the theoretical diagram have approximately the same values as the calculated maxima for a_2 and q_2.
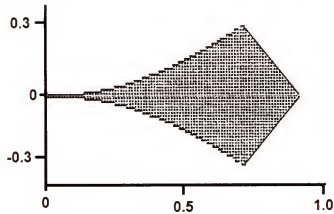
Figure 2.6. Calculated stability diagram for a quadrupole ion guide.

Figure 2.7 depicts the calculations for a hexapole ion guide (n=3). It should be noted that the upper boundary of the a_3 and q_3 parameters are greater in magnitude than the corresponding a_2 and q_2 boundary parameters for the quadrupole ion guide. This indicates that the stability region for a hexapole exists over a larger range of experimental values than the quadrupole ion guide.
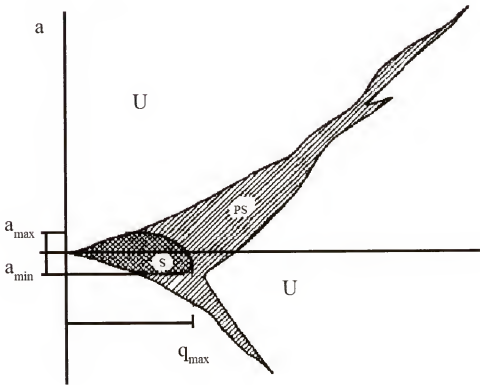
Figure 2.7. Theoretical stability diagram for a hexapole ion guide. U indicates unstable regions, PS indicates partially stable, and S indicates regions of stability.

This trend continues in figure 2.8, showing the calculated stability diagram for an octopole ion guide (n=4).
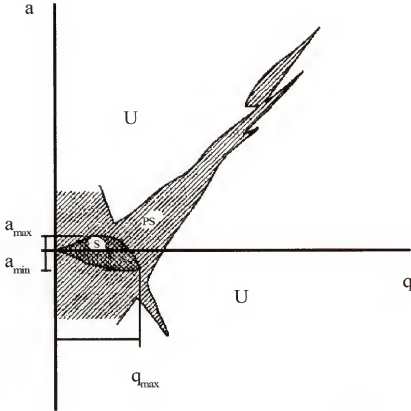
Figure 2.8. Theoretical stability diagram for a octopole ion guide. U indicates unstable regions, PS indicates partially stable, and S indicates regions of stability.

Table 2.1. compares the values of the a and q stability diagram parameters for each of the previous multipole diagrams.

A debate exists in the literature on the validity of the above equations. Gerlich spends several pages disputing the above theories based on his own concepts of adiabadicity.[24] While the Gerlich critique is very thorough, it is conceptually difficult to understand and to use to make predictions about ion behavior. Gerlich presents an adiabaticity parameter which can be used to predict stability to some extent. Matthieu stability parameters are even modified for the Gerlich version.

Table 2.1. Maxima and minima for a variety of multipoles with order n.[23]

n	a_{min}	a_{max}	q_{max}
2	-0.25	0.25	0.9
3	-1	1	6
4	-10	7	70

Note: All calculated values are approximate. a_{min} corresponds to the global minimum along the y axis for the calculated region of total stability. a_{max} corresponds to the global maximum along the y axis for the calculated region of total stability. q_{max} corresponds to the global maximum along the x axis for the calculated region of total stability.

This dissertation will use the theory expounded upon by Szabo, as it seems to be the standard theory used by other researchers in recent publications.[25-27] It should be noted that while Gerlich and Szabo may disagree on the details of ion motion in a multipolar ion guide, the Matthieu equations for a_n and q_n from each treatment contain ω in the denominator. This implies that mass selection can be accomplished by manipulating the applied rf frequency regardless of the theoretical basis.

As discussed earlier in this chapter, it is possible to select ions for transmission through a multipole ion guide by varying the applied DC and rf potentials, thereby modifying the a and q parameters. By far the most common procedure is to keep the amplitude and frequency of the applied rf voltage constant while varying the amplitude of the applied DC potential. This serves to keep q constant while changing the a parameter of the ions.

The amplitudes of the applied DC potentials are not the only parameters that can be changed to facilitate mass selection. Previous researchers have used rf frequency modulation to select specific ions passing through a quadrupole mass filter.[28,29] Since the frequency of the applied rf voltage appears in the denominator of the expression defining

the stability parameter, *q,* for multipole ion guides, it follows that decreasing this frequency for any multipole increases the *q* value, thus increasing the low mass cutoff. In this way only high mass ions are allowed to pass through the octopole ion guide.

Voyksner and Lee[30] coupled an octopole ion guide to a quadrupole ion trap for electrospray studies of milk extract. While this study showed the feasibility of the octopole as a high-pass mass filter, they observed only a ten fold increase in signal intensity. No previously undetectable signal appeared after ion preselection in the external octopole.

Guzowski and Hieftje[25] coupled a hexapole ion guide to a time-of-flight (TOF) mass analyzer for preselection of ions created by an inductively coupled plasma ionization source. Their research consisted mostly of varying the parameters on a external hexapole. While they saw an increase in mass resolving power for the TOF mass analyzer, they were not able to see a significant increase in sensitivity. In fact, detection limits for the external hexapole were comparable to those of static ion optics for their studies.

In the work described in chapters 3 and 4 of the dissertation, an external multipole ion guide was used as a mass filter for FTICR mass spectrometry. Removal of high abundance ions prior to transmission to the analyzer cell give rise to increased selectivity toward low abundance ions present in the sample. Ion accumulation concurrent with preselection could be used to further increase the sensitivity of the technique.

CHAPTER 3

GLOW DISCHARGE FTICR MASS SPECTROMETRY

Introduction

Glow discharge processes have found utility in mass spectrometry for the ionization of conducting and non-conducting solid samples. Plasma based methods are high energy ionization techniques that often atomize and ionize the sample. Since the samples are ionized there is the possibility of isotopic interferences, where isotopes of different elements have the same nominal mass. Ion- molecule reactions and incomplete atomization can lead to the production of isobaric interferences, where two atoms or molecules have the same nominal mass.

Many techniques have been developed to deal with these unwanted spectral interferences in elemental plasma sources. While these methods have shown varying degrees of success, the simplest way to deal with interferences is to separate their peaks directly from the desired analyte peaks using high or ultra-high resolution mass spectrometers.

Most commercial mass spectrometers used for elemental analysis employ either quadrupole or magnetic sector mass analyzers. While these instruments may offer various advantages in the analysis of samples by glow discharge, there is an inherent trade-off between resolution and sensitivity. Quadrupole mass filters are inherently low resolution devices, and narrowing the focusing slits in magnetic sector instruments

reduces sensitivity while increasing mass resolving power. One quite attractive alternative is to use a high resolution mass analysis technique that does not decrease sensitivity while acquiring high resolution spectra.

FTICR mass spectrometry is capable of achieving ultra-high mass resolving power in excess of 250,000 m/Δm[31] when coupled to a GD ionization source. The following section is designed to give an overview the glow discharge process as well as some advantages and disadvantages of performing GD FTICR mass spectrometry.

The Glow Discharge Process

Historically, the predecessors to the glow discharge phenomenon can be found in the 19th century research on gas discharges. Goldstein produced a report in 1886 on the presence of "luminous streamers" that traveled in the opposite directions of "cathode rays" composed of electrons. J.J. Thomson was the first to identify these luminous streamers as having a positive charge, and it is known that these are composed of positive ions.[32] Wein and Aston further characterized the positive rays produced by a glow discharge.[33] Dempster even produced what could be considered the first mass spectrograph.[34] These fundamental experiments on the nature of atomic constituents relied on glow discharges to create charged particles for analysis with electric and magnetic fields.

The glow discharge is quite simply a partially ionized gas consisting of a collection of equal numbers of positive and negative gas ions as well as neutrals. It is created by applying a potential across two electrodes, an anode (positive) and a cathode (negative), in the presence of a gas. At a sufficiently high voltage difference, breakdown of the gas occurs to produce a population of ions and free electrons. The behavior of the charged

particles is governed by the location and magnitude of the potential applied across the electrodes. In the case of the glow discharge, the free electrons are accelerated toward the anode, and the positively charged ions will be accelerated toward the cathode.

As a result of ion collisions with the cathode, the surface will undergo a phenomenon known as cathodic sputtering. Species ejected from the cathode during this process include neutral atoms, secondary electrons, ions, and various metastables. Neutral sputtered atoms can also undergo reactions with the other species to produce ions. Collisions with metastables and excited species can also result in the formation of ions in the glow discharge. Penning processes and electron impact are the two primary ionization sources. Charge transfer, cumulative ionization, associative ionization, and photon induced ionization are examples of secondary processes occurring in the glow discharge plasma. The dominating process in each experiment will depend heavily on the environmental conditions such as current, high voltage, pressure of the discharge gas, the geometry of the electrodes, and the geometry of the source housing used to create and sustain the glow discharge plasma. Table 3.1 lists the various reactions that correspond to each process mentioned above.

Three regions comprise the glow discharge. These are the cathodic dark space, the negative glow, and the Faraday dark space. At the surface of the cathode exists a large negative potential, repelling the electrons and attracting positive ions. This region near the cathode is not entirely devoid of electrons, due to the emission of secondary electrons from the cathode from collisions with accelerated positive ions. These electrons do not have sufficient kinetic energy for ionization and are considered 'slow' electrons.

Positive ions are attracted to the negative potential on the cathode as well as the electrons generated by secondary emission. This creates a dense population of positive

ions in a region just outside the dark space known as the negative glow region. The electrons in this region consist of high energy 'fast' electrons accelerated by the potential at the cathode, and slow electrons that have been cooled by collisions with background neutrals and other species.

Table 3.1. Ionization events in glow discharge plasma.[a]

I. Secondary Ionization Processes
  A. Charge Transfer
    1. Symmetric
      $X^0(slow) + X^+(fast) \rightarrow X^0(fast) + X^+(slow)$
    2. Non-symmetric
      $X^+ + M^0 \rightarrow M^+ + X^0$
    3. Dissociative
      $X^+ + MO \rightarrow M^+ + O + X^0$
  B. Cumulative Ionization
    $M^0 + e^- \rightarrow M* + e^- \rightarrow M^+ + 2e^-$
  C. Photoionization
    $M^0 + h\nu \rightarrow M^*/M^+ + e^-$
    $M* + h\nu \rightarrow M^+ + e^-$
  D. Associative Ionization
    $X^*_m + M^0 \rightarrow XM^+ + e^-$
II. Primary Ionization Processes
  A. Electron Impact
    $M^0 + e^- \rightarrow M^+ + 2e^-$
  B. Penning Process
    $M^0 + X^*_m \rightarrow M^+ + X^0 + e^-$
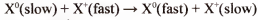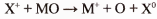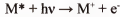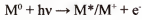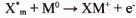
---
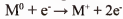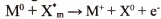
[a]M^0: sputtered atom, X^0: gas atom, M^+: sputtered ion, X^+: gas ion, M^*: sputtered metastable, X_m^*: gas metastable.[35]

Due to the abundance of electrons in this region, collisionally induced ionization and excitation are the predominant processes. The fast electrons have enough kinetic energy to produce ionization events in atomic and molecular species. Slow electrons can only ionize excited atoms or molecules or excite neutral species. The prevalence of excited state atoms and molecules in the negative glow is responsible for the bright glow characteristic of this region.

The next region is the Faraday dark space. The electrons have been cooled by inelastic collisions by the time they reach this region and do not have sufficient energy to produce ionization. The predominant species in this region are slow electrons moving toward the positive potential at the anode. This results in a low luminosity in this region.

Neutral ions sputtered from the cathode surface can be ionized by the processes described in table 3.1. Emission from excited state analyte atoms and ions sputtered from the cathode surface can be analyzed by spectroscopic methods. Unfortunately, spectral interferences can lead to complicated emission spectra. Of use in the experiments repeated here is the ability for the glow discharge to act as a solid sampling ionization source for a mass spectrometer. Analyte neutrals are sputtered directly from the cathode surface and ionized. To increase sensitivity, it is necessary to maximize the yield of sputtered analyte neutrals to make them available for ionization.

The choice of a sustaining gas can also be influential. A heavier gas will give a higher sputtering yield. A reactive plasma sustaining gas would also add additional spectral complexity and has the possibility of producing unforeseen products. Because of these conditions, noble gases are the most common choice for a plasma sustaining gas. Helium, neon, argon, and krypton are some of the various gases used to sustain the GD plasma.[36] While argon is one of the lighter noble gases, it is very cheap to purchase and has become the most common choice for glow discharge.

The most common glow discharge sources introduce samples by means of a direct insertion probe. In this configuration, the sample serves as the cathode and the GD cell housing serves as the anode. The probe and samples are introduced by means of a vacuum interlock system, usually a ball valve interlock. Other types of GD geometries include the Grimm style and the hollow cathode style.[35]

Glow Discharge Mass Spectrometry

Since the earliest methods for separating charged particles of different masses utilized positive ions created by a glow discharge, it can be said that the glow discharge ionization source is as old as the field of mass spectrometry. In contrast, the early analytical usage of a glow discharge was primarily limited to optical emission spectroscopy. The glow discharge provided another means for generating emission signal. The hollow cathode style lamp found utility in certain applications. To this day, glow discharge lamps are used as specific photon sources due to their stable operation and sharp line spectra. While optical methods suffer from the possibility of spectral interferences, mass spectrometry offers a viable solution to these problems. It wasn't until the work of Coburn and colleagues in the 1970's that coupling a glow discharge source to a mass spectrometer was realized.[37] Fortunately mass spectrometry does not suffer from as many interferences as optical spectroscopy, but it does have to deal with isobaric interferences.

Interferences

Isobaric interferences are defined as ions that have the same nominal mass as those corresponding to analyte species of interest. The most common type of isobaric interference is the isotopic interference, where isotopes of two different elements may overlap. Polyatomic interferences are the other type of isobaric interference and are caused by molecules with the same nominal mass as an analyte are also encountered in elemental analysis. The atomization step inherent to most elemental sources will often break up any molecules into their constituent elements. Therefore, polyatomic

interferences will often be formed by reaction or charge transfer with background species. Table 3.2 lists several examples of isotopic and polyatomic interferences and the mass resolving power needed to separate each.

Table 3.2. Mass Resolving Powers Required to Separate Several Atomic Ions and Potential Interferences

$m/\Delta m$	Interference	Atomic Ion	Atomic Ion Natural Abundance
18300	$^{62}Ni^1H^+$	$^{63}Cu^+$	69.20%
21300	$^{63}Cu^+$	$^{63}Ni^+$	Radioactive
35500	$^{106}Cd^+$	$^{106}Pd^+$	27.30%
57000	$^{74}Se^+$	$^{74}Ge^+$	36.50%
64400	$^{116}Cd^{16}O^1H^+$	$^{133}Cs^+$	100.00%
100000	$^{116}Cd^{16}O^1H^+$	$^{127}I^+$	100.00%
183000	$^{99}Ru^+$	$^{99}Tc^+$	Radioactive
193000	$^{40}Ar^+$	$^{40}Ca^+$	99.60%
319000	$^{238}U^+$	$^{238}Pu^+$	Radioactive
385300	$^{124}Sn^{16}O^1H^+$	$^{141}Pr^+$	100.00%
678000	$^{129}Xe^+$	$^{129}I^+$	Radioactive
825300	$^{124}Sn^{16}O^1H^+$	$^{139}La^+$	99.90%

Many techniques have been developed to deal with unwanted isobaric interferences in elemental plasma sources. Tanner was able to attenuate the argon and argon hydride ions in ICP MS by adjusting plasma conditions such as power and gas flow.[38] High-energy ion sampling,[39] modification of working conditions,[40] use of reactive gases in collision cells,[41-43] and low energy collision-induced dissociation (CID) for the dissociation of polyatomic species[44,45] have been used to remove unwanted interferences.

The most popular approach to reducing isobaric interferences in recent years seems to be the use of reactive gases in collision cells external to the mass analyzer. Various

gases are leaked into the ion transport system. The gases are chosen to be reactive toward one species in an isobaric pair. While this may seem useful, it adds an additional level of complexity to the sampling process. Reactions do not go all the way to completion in most cases. This means that there will often still be residual unreacted reactant as an isobaric interferent.

While the previously mentioned methods have shown varying degrees of success, the simplest way to deal with interferences is to separate their peaks directly from the desired analyte peaks using high resolution mass spectrometry.

Mass Analyzers

Once an ion population is formed by glow discharge, it is transported to the mass analyzer for measurement. The pressure in the GD source ranges from several hundred millitorr to several torr. Because of the high number of collision processes at these pressures, the kinetic energies of the ions created by GD are usually not high enough to cause serious difficulty when designing ion optics. This allows for the usage of common ion optics and ion guides for ion transport. Most importantly, the choice of a mass analyzer can greatly affect the type of spectra that can be obtained.

Quadrupole mass filters offer good sensitivity, but suffer from poor resolution. Their low cost and compact size have nonetheless made them a popular choice amongst researchers. Quadrupole ion traps offer better resolution at a similar cost and more compact size than the quadrupole mass filter. Unfortunately, they suffer from space charge limitations inherent to all ion trap devices.

Magnetic sector instruments can offer very high sensitivity and linear dynamic range, but to achieve good resolution it is necessary to decrease the widths of the various

ion collimating slits. To obtain the highest transmission efficiency, it is necessary to run the instrument in low resolution mode. Higher resolution modes call for the slits to be closed, hindering and reducing the transmission efficiency. Even with these disadvantages, the double focusing magnetic sector mass analyzer is a popular choice for elemental analysis.

When looking for high resolution, no other mass analysis technique can compare to FTICR mass spectrometry. The resolution of a typical FTICR instrument is often one to two orders of magnitude higher than that of any other mass analyzer. The mass resolving power and the mass accuracy can also increase even further with longer transient response times. Therefore, a larger amount of ions in the FTICR cell will produce a narrower, more accurate signal.

FTICR also offers several advantages such as Fellget's advantage and the ability to add together multiple time domain transient signals prior to Fourier transformation. This leads to enhanced sensitivity and signal-to-noise. Table 3.3 highlights some of the advantages and disadvantages for each type of mass analyzer.

GD-FTICR Mass Spectrometry

The first attempts to couple a glow discharge ionization source with FTICR mass spectrometry were in the late 1980's by Shohet and co-workers.[46] Marcus *et al.* were able to combine a rf-GD source to a 3.0T commercial mass spectrometer but were unable to achieve high resolution spectra.[47] Barshick and Eyler successfully coupled a high pressure DC glow discharge source to a laboratory built 2T FTICR mass spectrometer.[48] The high pressure in the cell due to the internal source led to diminished resolution and confirmed that this was not an ideal configuration for GD MS.

Table 3.3. Advantages and disadvantages for elemental analysis of several types of mass analyzers

Mass Analyzer	Advantage	Disadvantage
Quadrupole Mass Filter	-Tolerant of high pressures -Cheap to produce -Fast duty cycle -Compact	-Poor resolution
Time of Flight (TOF)	-Medium resolution -Theoretically simple -Good sensitivity	-Difficulty in ion extraction and pulsing
Quadrupole Ion Trap	-Medium resolution -CID can dissociate polyatomic interferences -Compact	-Disadvantages of ion traps (Space charge limitations)
Double Focusing Magnetic Sector	-Medium to high mass resolution -Good sensitivity	-Cost -Complexity -Trade off between sensitivity and resolution
FTICR	-Ultra-high mass resolution -No trade off between sensitivity and resolution	-Cost -Complexity -Large size -Dynamic range -Disadvantages of ion traps (Space charge limitations)

Watson and Eyler eventually converted the high pressure GD source to interface with a commercial instrument (Bruker, Billerica, MA) as an external source. The added stages of differential pumping helped to keep the base pressure in the analyzer cell far

lower relative to the internal source used in the previous experiments. Mass resolving power in excess of 200,000 was achieved with a NIST 1263a steel sample.[49]

In an attempt to further increase the mass resolution, a pulsed- gas glow discharge source was coupled to the commercial FTICR mass spectrometer. This instrumental setup allowed for further decrease of the gas load in the analyzer cell and mass resolving powers of 1.7 million m/Δm were achieved.[32]

It should be noted at this juncture that both Paul and Penning ion traps both suffer from space charge limitations. Due to the size limitations of the ICR cell, there is a limit on the total number of ions that may be stored and analyzed. Because only a small number of ions are required for detection, this is not a problem for most samples. It becomes a difficulty for samples where some of the analytes are in low abundance and other analytes or unwanted ions are in very high abundance. There may not be enough of the small abundance ions in the cell to permit detection.

This deficiency becomes especially significant when FTICR mass spectrometry is coupled to elemental ionization sources such as glow discharges. The typical solid elemental sample will only have trace amounts of many different elements. For an example we can look to the problem of contaminated concrete disposal.

Concrete is the most common building material in use at nuclear waste storage facilities. Due to the porous structure of concrete, any radioactive materials coming in contact with the concrete has the potential to be absorbed. A major objective of governmental cleanup effects is to prevent the complete destruction of these concrete structures. Removing only the contaminated layers requires an analytical testing method that can do depth profiling of solid samples, an ideal project for glow discharge mass spectrometry.

However, these samples are composed of large amount of low mass, high abundance species that may fill up the ICR analyzer cell with undesirable ions and prevent enough low abundance ions from being detected. It is possible to remove ions already in the analyzer cell with various shots, sweeps,[50] and stored waveform inverse Fourier transform (SWIFT) excitations. All of these techniques can be used to potentially isolate low abundance ions. But isolation does not involve enrichment, and ions that were undetectable before isolation will also be undetectable following these events.

One could imagine a series of successive accumulation/isolation steps where the low abundance species would be successively concentrated in the cell. This method would only be effective if the duty cycle were increased substantially. The number of successive steps would also be a limiting factor because different species would require a different number of steps.

A possible solution is to utilize the preselection methods discussed previously to remove any undesirable high abundance ions prior to introduction into the analyzer cell. In elemental mass spectrometry, it is likely that a majority of the sample will consist of lower mass ions, such as iron in a steel sample or copper and nickel in a brass sample. In the case of the concrete example discussed previously, the analyte ions would be high mass radioactive species. The majority of the sample would consist of oxides of silicon, calcium, and aluminum which are the major constituents of concrete (NIST SRM 1880 Portland Concrete).

Therefore, mass selection needs only be limited to operating the external ion guide as a high-pass mass filter. The high abundance ions will be removed thus allowing the low abundance ions to be concentrated in the FTICR analyzer cell.

Experimental

Glow discharge experiments were performed on a 3T FTICR instrument. The major hardware, vacuum system, and electronics were originally a Bruker Aspect 2000 FTICR Mass Spectrometer. The original Bruker data acquisition system was replaced with a laboratory built VXI-based data acquisition system. Detected signal was amplified by a differential preamplifier (Model:DA1822A, LeCroy, Chestnut Ridge, NY) and collected with an ADC/Filter (Model:E1437A, Hewlett Packard, Palo Alto, CA). Time domain data were processed using the MIDAS software[51,52] running on a desktop computer. The 3T system routinely had a base pressure of 3×10^{-8} torr during operation of the glow discharge source. The instrument was pumped by 4 different turbomolecular pumps. Three regions of differential pumping were provided, the analyzer region (56L/s and 330L/s), the ion optics region (800 L/s), and the octopole ion guide region (240 L/s). A schematic diagram on the instrument is shown in figure 3.1.
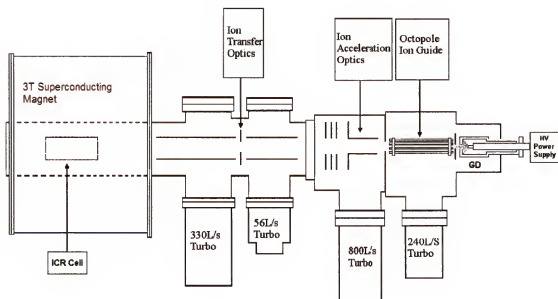
Figure 3.1. FTCR mass spectrometer used for GD experiments.

The cathode used in these experiments was a pin-type coaxial cathode mounted on the end of a direct insertion probe. The anode was a grounded high pressure compartment with a 1mm ion transmission orifice, identical to the system used in previous studies with external dc-GD FTICR-MS.[32] The GD source transmission orifice was located in line with the ion lens stack of the Bruker FTICR instrument with a spacing of approximately 10 mm between the transmission orifice and the first ion lens. Samples were mounted on the end of the direct insertion probe and consisted of metal rods 1-4 mm in diameter and 20-30 mm in length. For each sample, the probe distance from the transmission orifice was varied until maximum signal was produced. DC voltage was supplied by a high voltage power supply (Model:210-10R, Bertan Associates, Inc.,Valhalla, NY). A dc voltage of -1.0 to -1.6 kV was applied to the cathode. Higher voltages led to an undesirable arc discharge between the anode and the cathode. A schematic representation of the source is shown in figure 3.2.
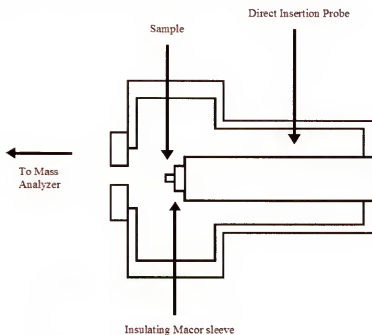
Figure 3.2. Schematic of the coaxial cathode type GD source used in the experiments.

Argon (99.9%) was used as the plasma sustaining gas in all experiments. Argon was introduced into the high pressure compartment through a variable leak valve (Model:203, Granville-Phillips Co., Longmont, CO). Source pressures ranged from 0.8 to 1.0 mTorr. Higher source pressures resulted in a higher background pressure in the analyzer cell, effectively decreasing the resolution of the instrument.

A laboratory built octopole was interfaced to the mass spectrometer to provide an ion guide for mass filtering as well as an additional region of differential pumping. A synthesizer/frequency generator (Model: 3325B, Hewlett Packard, Palo Alto, CA) and an rf power amplifier (Model: 2100L, ENI Products, Rochester, New York) were used to provide rf power to the octopole. Figure 3.3 shows an electrical circuit diagram of the components used to couple rf and dc voltages to the octopole rods. It should be noted that the electrical system was designed to provide a differential dc bias to each of the two sets of four octopole rods. Voltages were applied by several dc power supplies.

Results

The first experiments involved testing the parameters of the dc-GD source with the laboratory built octopole ion guide to determine the optimal parameters for octopole operation as well as optimal distance between the GD source and the entrance of the octopole. A small copper plate with a thickness of approximately 0.25 mm was placed in between the second ion optic at the analyzer side of octopole and the first lens on the Bruker ion optic stack. This plate was connected to an electrometer and the induced ion current was measured. Positive ions produced by the GD source would pass through the octopole and collide with the copper plate. The positive ions would be neutralized, resulting in a current. If the octopole ion optics were set to sufficiently high positive dc
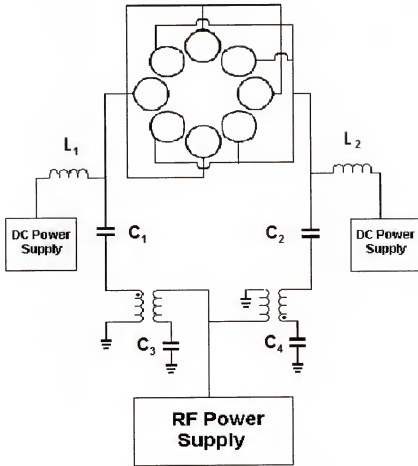
Figure 3.3. Electrical circuit used to provide power to the octopole rods. $C_1 = C_2 = 33\ \mu F$, $C_3 = C_4 = 50nF$, $L_1 = L_2 = 3.9$ mH, transformers are 100 W Balun transformers (Model:0704BB, North Hills Signal Processing, Syosset, NY). The octopole was 0.75 inches in diameter and 8 inches long. Octopole spacing not to scale.

potentials, the ion current would decrease to zero.

Typical magnitudes for ion currents exiting the octopole ranged from 10^{-8} to 10^{-9} amperes. From these experiments it was determined that maximum ion current was inversely proportional to the distance between the entrance ion optic on the octopole and the GD source housing. This placed a limitation on the magnitude of the potentials that could be placed on the entrance optic to the octopole. High voltages would result in an

electrical discharge between the entrance ion optic and the GD source housing, which was grounded. It was determined that the distance was more important than high voltages applied to the ion optics on either side of the octopole ion guide. Due to these results, the GD source housing was placed 5 mm from the entrance ion optic.

Initial mass spectrometry experiments focused on testing the coaxial cathode and GD source on the 3T FTICR mass spectrometer. These studies were carried out without the octopole ion guide and involved no preselection. The GD ionization source was coupled directly to the mass spectrometer so that the exit orifice for the GD source was 5-8 mm from the first Bruker ion optic. This is a typical distance for the other ionization sources used on the 3T instrument.

Previous studies in our laboratory had been confined to copper, brass, and steel samples.[32,46]

Figure 3.5 depicts spectra obtained from pin samples of tantalum, indium, and iron.
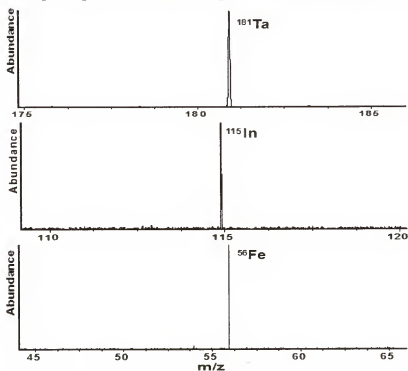
Figure 3.4 GD FTICR mass spectra obtained from pin samples of Ta, In, and Fe.

These spectra were obtained with very little change in GD experimental parameters from the earlier studies. The intent was to show that FTICR mass spectrometry can acquire spectra with good S/N for a wide variety of samples other than the standard copper samples seen later in this study. This indicates that the GD ionization source may have utility for physical chemistry studies. FTICR is renowned as a powerful tool for the study of gas phase ion-molecule reactions. GD has the potential to be a robust source of metal ions for reactions of this type.

dc-GD with Octopole

Copper samples were used for tuning and optimization of instrumental parameters after the octopole ion guide was inserted between the GD source and the Bruker instrument. Initial preselection experiments involved keeping the rf frequency constant and varying the dc offset on the octopole rods. Relevant parameters were varied over a wide range, but no conditions were found that would give significant attenuation of the low mass ions while transmitting a reasonably high current of high mass ions. Some decrease in signal intensity for high abundance ions was seen but it was often accompanied by a decrease in signal intensity for the low abundance ions. Since the purpose of this study was to prevent the loss of low abundance ions, this was undesirable.

Variation of the frequency of rf voltage applied to the octopole rods was next attempted. In these experiments, the octopole frequency was slowly decreased while keeping the other parameters constant. Based on the theory discussed in previous chapters, as the frequency decreases, the octopole ion guide should act as a high-pass mass filter.

Figure 3.5 shows the results of using frequency variation to preselect ions created

by dc GD.
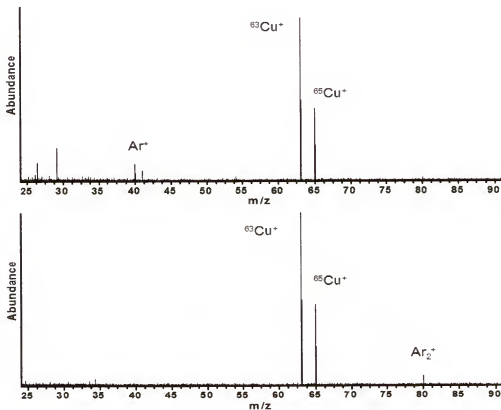
Figure 3.5. Glow discharge FTICR mass spectra of a copper sample showing the effects of preselection on low abundance ions. The rf frequency applied to the octopole rods of the top spectrum was 1.75 MHz, for the bottom spectrum it was 850 kHz.

The two spectra in figure 3.5 were obtained no more than five minutes apart,

without changing any of the FTICR acquisition parameters; only the frequency of the rf

voltage applied to the octopole was changed.

If the frequency was lowered to values nearer to 600 kHz, all signal disappeared

from the spectrum. This is consistent with the theoretical treatment since even the high

mass ions should eventually be lost as the low mass cutoff of the octopole moves to

increasingly higher masses as the rf frequency applied to the octopole decreases.

After promising results with copper and iron, a NIST brass sample (SRM 1104) was
prepared and analyzed using the DC GD preselection technique(Figures 3.6 and 3.7).
This sample was chosen because it contained several high mass analytes in low
abundance. The high abundance analytes were copper and zinc, composing 96.7%
percent of the sample. Initial results showed a very large signal for copper and zinc, the
two primary components of brass. A small signal was also observed for lead, which was
present in 2.77% abundance in the sample. No other signal was observable above m/q 60
other than the copper, zinc, and lead.
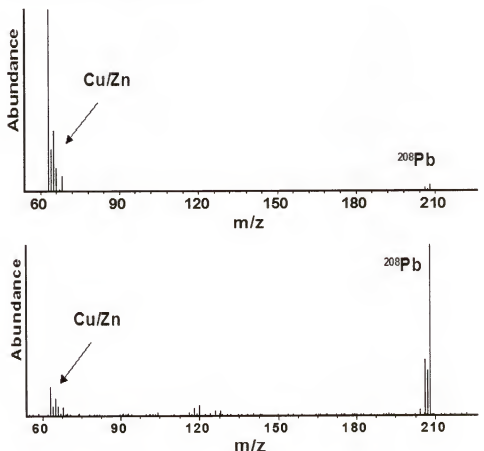
Figure 3.6. Spectra of a brass sample (NIST 1104) showing the effects of
preselection on low abundance ions. The rf frequency applied to the octopole rods for the
top spectrum was 1.9 MHz, while the rf frequency of the bottom spectrum was 660 kHz.
An increase in signal intensity for lead (2.77% abundant) relative to copper (61.33%
abundant) and zinc (35.31% abundant) is seen. Ion accumulation time was 2 seconds in
the top spectrum, and 6 seconds in the bottom sample.

It proved difficult to remove all high abundance ions while retaining a good signal-to-noise ratio for all detected signals. This can be attributed to the fact that the operational parameters of the octopole were very close to the boundary for ion stability. The ion accumulation time was doubled to obtain the octopole preselection spectra. This served to accumulate the high mass ions in the analyzer cell.
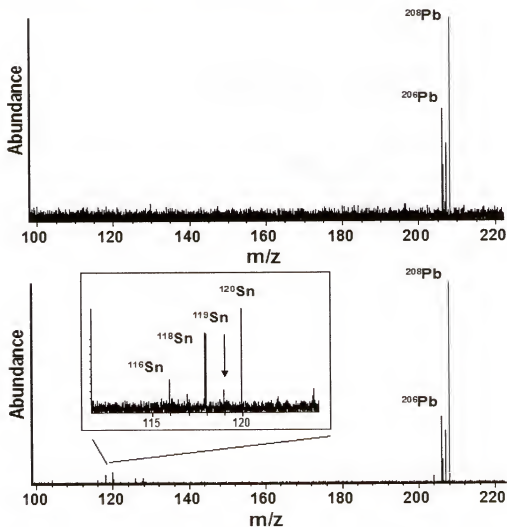
Figure 3.7. Spectra of the NIST 1104 brass sample seen in figure 3.5. Tin (0.43% abundant) can be seen above the noise in the bottom spectrum. The mass range was expanded over the 100-220 m/q range to show detail. Note that the tin ions were not observable in the top spectrum. The frequency of the applied rf was identical to the conditions shown in figure 3.6.

Nevertheless, the removal of a large amount of the high abundance ions should

still allow for increased sensitivity toward low abundance ions. Table 3.4 lists the

certified composition of the NIST brass sample.

Table 3.4. The certified composition of NIST SRM 1104, free-cutting brass pin sample.

Element	Percent Composition in Sample	Isotopic Distribution[†]
Cu	61.34%	[63]Cu (69.17%) [65]Cu (30.83%)
Zn	35.36%	[64]Zn (48.6%) [66]Zn (27.9%) [68]Zn (18.8%)
Pb	2.72%	[204]Pb (1.4%) [206]Pb (24.1%) [207]Pb (22.1%) [208]Pb (52.4%)
Sn	0.42%	[116]Sn (14.54%) [117]Sn (7.68%) [118]Sn (24.22%) [119]Sn (8.59%) [120]Sn (32.59%) [122]Sn (4.63%) [124]Sn (5.79%)
Fe	0.087%	[54]Fe (5.85%) [56]Fe (91.75%) [57]Fe (2.12%)
Ni	0.073%	[58]Ni (68.08%) [60]Ni (26.22%) [61]Ni (1.14%) [62]Ni (3.63%)
Ph	0.005%	[31]P (100%)

[†]Isotopic percent abundance shown in parentheses. Isotopes with a natural abundance less than 1.0% are not not shown. Data taken from the SRM certification data sheet.

By comparing peak heights of the copper and zinc signals in the two spectra, significant attenuation of the low mass ions can be seen. Additionally, an increase in Pb signal relative to the background is apparent, and Sn signal becomes visible. The

appearance of the previously undetected Sn after preselection validates the power of this technique to increase the sensitivity of GD FTICR mass spectrometry toward low abundance ions in a solid sample. As in the previous experiments, sweeping the frequency applied to the octopole toward lower values caused the low mass cutoff bandpass of the octopole to move to higher and higher masses. Subsequently, the applied RF reached a frequency where all the analytes were preselected and no signal was detected, consistent with theory.

To achieve the sensitivity, long accumulation times were used to further concentrate the low abundance ions in the FTICR analyzer cell. Accumulation times on the order of 3.0-8.0 seconds were typical for experiments using preselection. Normal accumulation times without preselection ranged from 0.5-2.0 seconds.

It should be noted that little or no signal for argon was detected when the instrumental parameters were optimized for maximum sputtered ion intensity. The decreased intensity of argon relative to that of the sputtered ions could be due to several factors. Firstly, the ion transfer optics may have been optimized for higher mass ions and not the lower mass ions. This is unlikely because a small signal for water was sometimes observed.

Secondly, ultra high purity argon was not used in these experiments. The effects on analyte signal intensity between ultra high purity argon and 99% purity argon was investigated in early experiments of this research. It was discovered that using the ultra high purity argon did not have a significant effect on the analyte signal. Using a lower purity argon did seem to cause a decrease the background Ar^+ signal. This is possibly attributable to the impurities present in the lesser purity argon or a leak in the inlet system. A recent study by Hastings and Harrison[53] found that small amounts of

impurities in the argon plasma sustaining gas can lead to a significant decrease in the Ar^+ signal, while the analyte signal showed only a very small decrease in signal intensity. This could explain the decreased intensity of the argon signal.

Conclusions

The combination of a glow discharge (GD) ionization source with external preselection for Fourier transform ion cyclotron resonance (FTICR) mass spectrometry has resulted in increased sensitivity for analysis of high mass, low abundance ions. The sample investigated was a National Institutes of Standards and Technology (NIST) free-cutting brass standard, SRM 1104. Study of this standard revealed mass spectral peaks of Pb that was in 2.8% abundance (by weight) in the sample. When external preselection of the high abundance ions was implemented, previously unseen mass spectral peaks were resolved of the isotopes (14.54%, 24.22%, and 32.59% natural abundance) of tin that was present in 0.42% abundance (by weight) in the sample. These data demonstrate the power of external preselection to improve the selectivity of GD FTICR mass spectrometry for low abundance analytes in the presence of extraneous high abundance analytes or background. While the mass resolving power of the octopole is lower than that of a quadrupole, this research shows potential for applying this technique to instruments with existing multipoles that are acting solely as ion guides. The preexisting multipole ion guides could then be used as high-pass mass filters simply by decreasing the frequency of the applied rf voltage.

This approach can also be applied to environmental and materials samples where the analyte of interest is almost always in low abundance. However, this technique could

prove to be even more beneficial when applied to inductively coupled plasma (ICP)

ionization sources or even non-plasma based ionization sources.

CHAPTER 4
ELECTROSPRAY IONIZATION FTICR MASS SPECTROMETRY

Introduction

Electrostatic charging can be used to generate a fine mist of droplets from a
solution through a process known as electrospray (ES). The application of a high voltage
potential electrically charges the solution. As the solution droplets are forced to hold
more and more charges, they become unstable. Once the charge reaches the Rayleigh
limit[54] the rf forces exceed the surface tension. The solution is then broken up into a fine
mist of charged particles.

Evaporation will occur from these small droplets, causing further fission due to
concentration and repulsions of the charges. By placing a potential of opposite polarity
nearby, the charged droplets can be forced to migrate to a desired location. This
technique has found usage in industrial application as the fine mist of droplets can be
used to coat a surface with paint or other materials.

In the last ten years, electrospray methods have become very popular as a source of
ions for mass spectrometry. In this technique, a solution is placed in a hollow tube and is
forced out using a syringe pump. The tube, called the needle, is positioned near the
sampling inlet to the mass spectrometer and a large potential is applied between the
needle and the inlet.

The solution passes through a narrow orifice at the tip of the ES needle. After the
potential is applied to the tube, ions in the solution migrate to the tip of the needle. This

results in the formation of the Taylor cone, a liquid cone formed by the movement of charge in the body of the needle. By choosing the appropriate polarity to apply to the tube, the charged droplets can be made to move from the tube toward the mass spectrometer inlet.

Passing the droplets through a region of increased temperature, typically a heated capillary operating at several hundred degrees Celsius, results in increased desolvation efficiency. As the droplets continue their desolvation, ions are eventually produced. The specific mechanism by which ions are created by the ES process is still in contention amongst the scientific community.

ES ionization is considered to be a "soft ionization" technique, that is little or no fragmentation is produced during the ionization process. While this decreases the amount of structural information available, it does allow for large molecules to be ionized while retaining higher order structure. Other methods, such as collision induced dissociation (CID)[55] and infrared multiphoton dissociation (IRMPD)[56], can be used to induce fragmentation prior to analysis.

The ES ionization technique also has the ability to produce multiply charged species. The resulting decrease in the m/q of large molecules makes this technique especially valuable for the analysis of large molecular weight species. Coupled with high resolution mass analyzers such as FTICR, ES ionization has become an increasingly popular technique for the analysis of large biomolecules.

Depending on the chemical structure of the molecule, some species may have a large number of multiple charge states. Unfortunately, this only adds to the complexity of the mass spectrum. Ions present in high abundance will quickly fill the FTICR analyzer cell, leaving little room for low abundance species. Due to the space charge effects

discussed in the previous chapter, some low abundance charge states produced by ES ionization may not be present in high enough concentration to allow for analysis by FTICR mass spectrometry. Given success with the glow discharge ionization source, it was decided to extend experiments involving preselection to the ES ionization technique.

Experimental

Electrospray experiments were performed on a 4.7T FTICR instrument. The major hardware, vacuum system, and electronics were originally part of a Bruker Apex 47e FTICR Mass Spectrometer. The original Bruker data acquisition system was replaced with a homebuilt VXI-based data acquisition system.[51,57] Detected signal was amplified by a differential preamplifier (Model:DA1822A, LeCroy, Chestnut Ridge, NY) and collected with an ADC/Filter (Model:E1437A, Hewlett Packard, Palo Alto, CA). Time domain data was processed using the MIDAS software running on a desktop computer.

The 4.7T system routinely had a base pressure of 2×10^{-9} torr during operation of the electrospray source. The instrument was pumped by 4 different turbomolecular pumps. Three regions of differential pumping were provided, the analyzer region (70 L/s and 500 L/s), the ion optics region (500 L/s), and the electrospray source region. (240 L/s).

The electrospray source was a commercial Analytica source modified with a heated metal capillary.[58] The source consists of four major parts. The first part is the electrospray needle assembly. The needle is mounted in a grounded box that pulls out to enable inspection and changing of the needle. A high voltage is applied to the needle to facilitate the electrospray process.
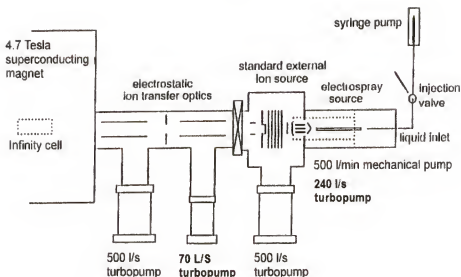
Figure 4.1. Instrumental schematic of the modified Bruker Apex 47e with a modified Analytica electrospray source.

The fine mist of charged droplets and ions created by the electrospray process passes through a heated metal capillary to enhance desolvation. This capillary is routinely kept at 150^0 C and is heated resistively by an external power supply. A thermisistor is used to measure the temperature of the heated metal capillary and a feedback loop circuit is used to maintain a constant temperature over the course of the experiments.

After the ions leave the capillary, they reach a region pumped by a 500 L/min mechanical pump. Ions then pass through a skimmer cone, to reach another region of differential pumping where the vacuum is maintained by the 250 L/s turbomolecular pump.

After passing through the skimmer cone, ions enter a 10 cm long hexapole ion guide. The skimmer cone and an annular disc located at the ends of the hexapole can be

used to trap the ions inside the ion guide by the application of a sufficiently large potential. The magnitude of this potential is experiment dependent. These two optics were used for ion accumulation in the hexapole prior to transferring the ions to the analyzer cell and are shown in figure 4.2. In the experiments described in this chapter, ions were accumulated for 0.5 seconds.
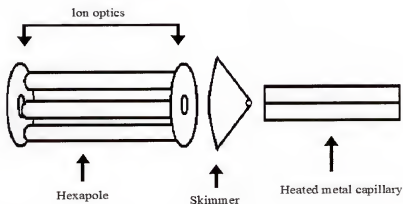
Figure 4.2. Ion optics in the modified Analytica ESI source. The ion optics at either end of the hexapole ion guide are used for ion accumulation. The hexapole is 0.95 inches and 0.15 inches in diameter. Only three rods on the hexapole are shown for clarity.

Longer accumulation times produced no significant improvement of ion peak heights, presumably due to space charge limitations in the relatively narrow hexapole. All of the ion optics for the Bruker instrument and the Analytica source were controlled by a Windows based software program developed by Prof. David Dearden at Brigham Young University. This program provides a graphical interface that can be used to control the ion optics on the Bruker system. This program does not control the amplitude or frequency of the rf applied to the hexapole ion guide. 5 MHz is the frequency applied to the hexapole during normal operating mode.

To allow control over the rf parameters, a synthesizer/frequency generator (Model: 3325B, Hewlett Packard, Palo Alto, CA) and an rf Power Amplifier (Model:

2100L, ENI Products, Rochester, New York) were used to provide rf power to the
hexapole. The Analytica source used a specialty electrical plug made by Fischer
Connectors that was designed to interface between the rf power supply and the hexapole.
Fischer Connectors was contacted and they not only supplied information about the
connections, but they also donated a replacement specialty plug to the researchers. The
donated plug was used to connect the frequency generator/power amplifier to the
hexapole.

Results

A 6 μM solution of human Angiotensin II in 50% MeOH/49% H_2O/1% HOAc was
chosen as the first sample to be analyzed with hexapole preselection. Angiotensin I is a
peptide with the sequence Asp-Arg-Val-Tyr-Ile-His-Pro-Phe-His-Leu. The peptide is
cleaved between Phe and His by the Angiotensin Converting Enzyme to form
Angiotensin II. While Angiotensin I has no physiological effects, Angiotensin II is a
vasoconstrictor with several functions in the body.

The solution used for these experiments was used by other researchers in the
laboratory as a test solution used for tuning the instrument because it produced very
intense ion peak heights. Instrumental and experimental parameters could then be
optimized on this test solution before unknown samples were analyzed. Unfortunately,
the solution was contaminated with a high concentration of acetate clusters, producing a
very large peak at m/q 538. This is a common contaminant composed of acetate clusters
found in samples prepared with acetic acid.[59] As evidenced by the spectrum in Figure
4.3, these acetate ion clusters were the most prominent signal obtained.
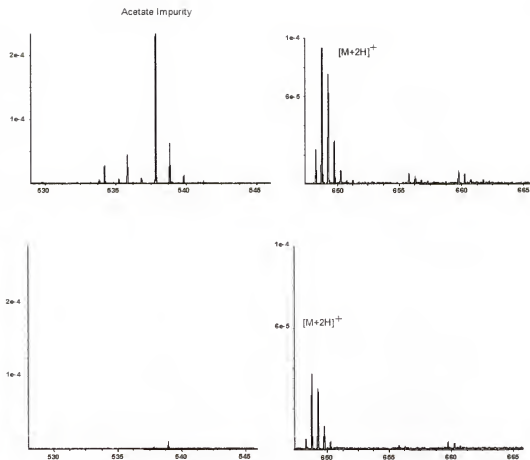
Figure 4.3. ESI FTICR mass spectra of a contaminated 6 μM Angiotensin II solution. Each mass range shows the two most prominent clusters of peaks in the entire mass spectrum. The sample was run at a flow rate of 17.5 μL/hr. The hexapole operational frequency was 3.4 MHz for the top spectrum and 1.9 MHz for the bottom spectrum.

The 1+ charge state of Angiotensin II was not visible when using the solution. This made the sample unsuitable for tuning instrumental parameters for high mass ions, as no ions above 650 m/q were visible in the spectrum. By slowly decreasing the frequency of the applied rf to the hexapole, it was possible to decrease the ion peak height of the acetate clusters. Figure 4.4 and 4.5 presents the results of operating the hexapole at a different frequency. The signal due to the acetate cluster was eventually removed

completely and a new signal appeared from the noise. As shown in figure 4.3, the new signal was the 1+ charge state of Angiotensin II.
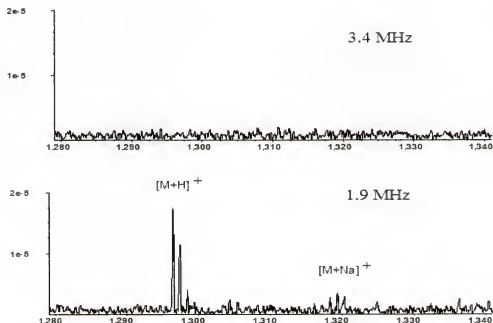
Figure 4.4. High mass range from the spectra in Figure 4.3. The hexapole operational frequency is 3.4 MHz in the top spectrum and 1.9 MHz in the bottom spectrum. No other operational parameters were changed between the acquisition of each spectrum. Each spectrum is a sum of 64 scans.

After seeing the appearance of the previously undetected charge state, an experiment was run over a series of four different applied rf frequencies to depict the amount of low mass ion attenuation due to ion preselection in the external multipole. Figure 4.5 presents the results of this experiment. The lowest frequency used was 1.5 MHz, which also corresponds to the lowest frequency of the applied rf voltage for which signal could be obtained. At frequencies below 1.5 MHz, no signal was observable even with significant ion accumulation in the analyzer cell.
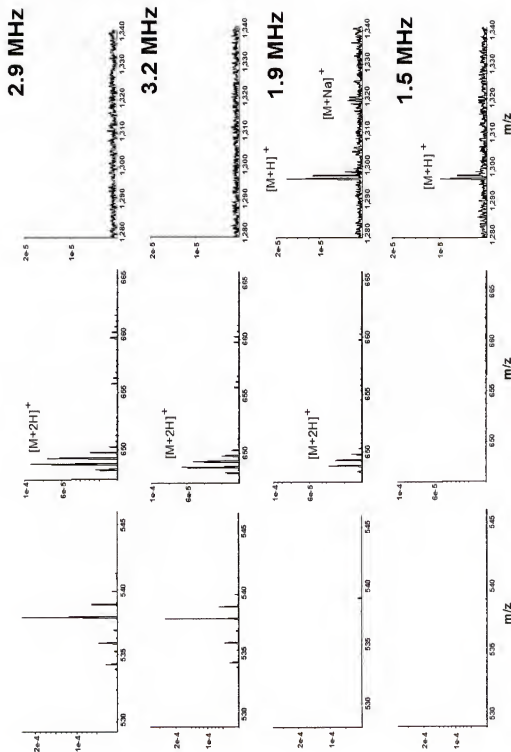
Figure 4.5. ESI FTICR mass spectra of a contaminated 6 μM Angiotensin II solution. Each column consists of several zoomed in slices of a single spectrum. The frequency of the applied rf for each spectrum is listed to the left of each row. The Y-axis scale is consistent across each row, but not down the columns.

The S/N values for each peak were obtained by examining the absolute peak height values for each peak to determine the signal intensity. The signal intensity was then divided by the mean absolute intensity for a series of background noise peaks at the base of each signal peak to produce the S/N values listed by the graph. Figure 4.6 shows a comparison of the signal to noise values for a series of spectra collected at various frequencies of the applied rf voltage.
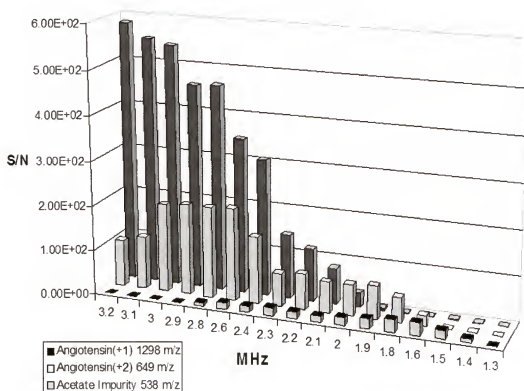
Figure 4.6. S/N comparisons in the Angiotensin spectra for a variety of hexapole operational frequencies. Each spectrum is a sum of 64 scans.

The next system studied by this technique was a sample of Agilent tune mix (PN G2422A). This is a proprietary premixed solution of compounds developed by Agilent

Technologies for use with their liquid chromatography mass spectrometers. Table 4.1 lists the major peaks found in this mixture. This sample was chosen because it contained a mixture of several ions that covered a wide range of m/q values. It would then be possible to observe the effects of changing the frequency of the applied rf voltage to the hexapole over a wide mass range. In past experiments by researchers in the laboratory, only the peaks at 622.03, 922.01, and 1521.9 could be detected.

Table 4.1. Major Ions found in PN G2422A.

m/q
622.03
922.01
1521.9
2121.9
2721.9

Figure 4.6 is a combination of four spectra obtained over a 5 minute period of a tenfold dilution of the original Agilent tune mix stock solution. The original solution was found to be far more concentrated than was needed, and even a tenfold dilution produced large signal for analysis.

By comparing the absolute intensity of each of the peaks in the above spectrum, it can be seen that the low mass ions are in the highest abundance. As the frequency of the applied rf is decreased, the low mass ions are attenuated until they are removed completely from the spectrum. The signal at m/q 2121.9 was previously undetectable by other researchers on the instrument used in this study.
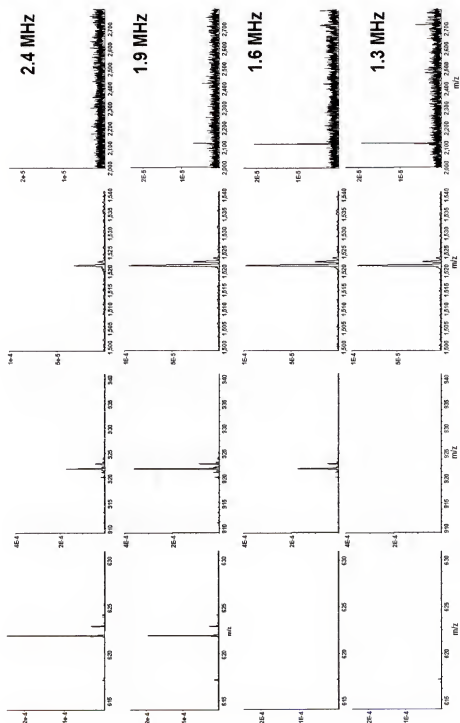
Figure 4.7. ESI FTICR mass spectra of a 10 fold dilution of Agilent Tune mix. Each column consists of several zoomed in slices of a single spectrum. The frequency of the applied rf for each spectrum is listed to the left of each row. The Y-axis scale is consistent across each row, but not down the columns.

Conclusions

The combination of ion preselection in a external hexapole ion guide with FTICR mass spectrometry has resulted in the ability to see previously undetectable high mass ions. This research has proved that a commercial instrument can be modified to quite easily allow ion preselection. Samples included a contaminated sample of human Angiotensin II and a commercially available calibration mixture. Analysis of both samples proved that ion preselection could be used to attenuate low mass, high abundance ions and improve the signal to noise of high mass, low abundance ions. The resulting data demonstrate the potential capabilities of ion preselection for complex samples. However, additional work is needed for improvements in this subject such as accumulation with multiple applied rf frequencies so as to include some of the low mass ions in the analyzer cell along with the high mass ions.

CHAPTER 5

ATMOSPHERIC PRESSURE PHOTOIONIZATION

Introduction

As discussed in a previous chapter, electrospray ionization is a soft ionization method. It can ionize samples with little or no fragmentation, allowing molecular ions to retain much, if not all, of their structural identity. Electrospray is not the only soft ionization technique available to researchers. Other methods are atmospheric pressure chemical ionization (APCI) and atmospheric pressure photoionization (APPI).

Atmospheric Pressure Chemical Ionization

APCI development dates back to the first atmospheric ionization source developed by Horning, *et al.* in the early 1970's.[60,61] They used both a ^{63}Ni ionization source and a corona discharge to ionize a mixture of analyte and solvent molecules from either a gas chromatography (GC) or a liquid chromatography (LC) source. The solvent was specifically chosen to assist in ionization as a chemical ionization (CI) reagent. The most common ion in APCI mass spectrometry is the protonated parent ion peak $(M+H^+)$ ion and unlike ESI, multiply charged species are not common.

The protypical APCI ionization source is composed of three main parts. The first is a pneumatic nebulizer, consisting of a capillary by which the solvent/analyte mixture is sprayed from a nozzle surrounded by a concentric nebulizing gas flow. The second part

is a heated tube used to aid in the vaporization of the droplets produced by the solution passing through the nozzle. This tube, although not part of the nebulizer assembly mentioned above, is often referred to as the heated nebulizer when used in combination with the pneumatic nebulizer. The final piece of the APCI assembly is a corona discharge needle. The corona discharge is a plasma that serves to facilitate a series of reactions leading to ionization of the analyte.

Using nitrogen as a nebulizing gas and a background amount of water, the following reactions are the primary and secondary reactions found in the corona discharge.[62]

Table 5.1. Summary of some possible reactions in a corona discharge.

$$N_2 + e^- \rightarrow N_2^{+\bullet} + 2e^-$$
$$N_2^{+\bullet} + 2N_2 \rightarrow N_4^{+\bullet} + N_2$$
$$N_4^{+\bullet} + H_2O \rightarrow H_2O^{+\bullet} + 2N_2$$
$$H_2O^{+\bullet} + H_2O \rightarrow OH^\bullet + H_3O^+$$
$$H_3O^+ + H_2O + N_2 \rightarrow [H^+(H_2O)_2] + N_2$$
$$[H^+(H_2O)_{n-1}] + H_2O + N_2 \rightarrow [H^+(H_2O)_n] + N_2$$
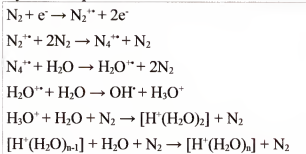
Based on work by Sunner and Kebarle[63,64] it has been determined that a potential ionization path is proton transfer from the water clusters in the above reactions. Another ionization path is through charge exchange with ionized solvent molecules or solvent molecule clusters.[65] Either of these do not easily allow for the ionization of less polar or nonpolar molecules, as most molecules of this type have low proton affinities and high ionization energies relative to other analytes. This leads to decreased sensitivity for these types of molecules.

Atmospheric Pressure Photoionization

Another potential option for ionizing less polar and nonpolar species is atmospheric pressure photoionization(APPI). Developed for atmospheric pressure mass spectrometry in 2000 by Robb, Covey, and Bruins,[66] photoionization is the youngest of the soft atmospheric pressure ionization techniques. Figure 5.1 compares the optimal regimes for ionization between several different atmospheric pressure photoionization techniques.
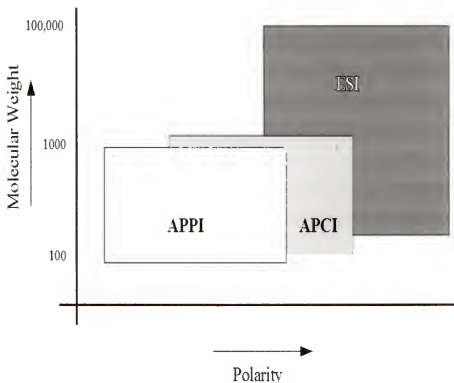
Figure 5.1. General comparison of Important Factors for APPI, APCI, and ESI.

species, then ions are formed. Table 5.2 lists the most important of the many reactions involved in the APPI process. Photoionization in APPI takes place in the gas or condensed phase. Photons emitted from a UV source interact with solvent and analyte molecules and form excited species. If the energy of the photon is greater than the ionization energy of excited species, then the molecules can be ionized

Table 5.2. Reactions found in the APPI ionization source.

Photoexcitation	$AB + h\nu \rightarrow AB^*$
	$S + h\nu \rightarrow S^*$
Photodissociation	$AB^* \rightarrow A + B$
Radiative Decay	$AB^* \rightarrow AB + h\nu$
Collisional Quenching	$AB^* + S \rightarrow AB + S^*$
Ionization	$AB^* \rightarrow AB^{+} + e^-$
Recombination	$AB^{+} + gas + e^- \rightarrow AB + gas$
	$AB^{+} + S + e^- \rightarrow AB + S$
	$AB^{+} + e^- \rightarrow AB$

Note: AB is an analyte molecule, S is a solvent molecule, gas is a background gas molecule, and AB* and S* are the respective excited state molecules for AB and S.

If the aforementioned UV source is chosen so that the energy of its emitted photons is lower than the ionization energies of the solvent molecules and higher than the ionization energies of analytes, it is possible to discriminate between the ions formed by photoionization so that only analyte molecules are photoionized. It is therefore possible to eliminate the potential phototionization of solvent molecules by choosing a photoionization lamp that emits sufficiently high energy photons. Typical discharge lamps used for photoionization include argon (11.2 eV photons), krypton (10.0 eV), and xenon (8.4 eV). Of the three, krypton lamps are the most common due to the fact that energy of its emitted photons are less than the ionization energies of air and many common solvents while still having a photon energy higher than the ionization energy of most most aromatic molecules. Table 5.3 lists the evaluated gas phase ionization energies of some common solvents.[67-77]

Table 5.3. Gas Phase Ionization Energies of some Common Gases and Solvents

Compound	Ionization Energy (eV)
Nitrogen	15.58
Water	12.62
Acetonitrile	12.2
Oxygen	12.07
Methanol	10.84
Isopropanol	10.17
Hexane	10.13
Acetone	9.7
Pyridine	9.25
Benzene	9.24
Toluene	8.83

The majority of the photon flux in APPI involves reactions with solvent molecules due to the high proportion of solvent molecules relative to the analyte. Because of the lower concentrations of the analyte, is it less likely to interact with the available photon flux One possible solution to this dilemma is the addition of another compound, known as a dopant, that serves to increase the number of analyte ions. The dopant is a compound that has a low proton affinity or an ionization energy lower than the emission photons of the photoionization lamp. The dopant acts as an intermediate between the photons and the analytes by being photoionized and then ionizing the analyte by charge transfer or proton transfer. The most common dopants seen in the literature are acetone and toluene, usually added post-column if APPI is used for a chromatography experiment.

Table 5.4 lists several possible reactions between the dopant molecule and the analyte molecule during APCI.

Table 5.4. Reactions involving dopant in the APPI ionization source.

Ionization	$D + h\nu \rightarrow D^{+\cdot}$
Charge Transfer	$D^{+\cdot} + AB \rightarrow AB^{+\cdot} + D$
Proton Transfer	$D^{+\cdot} + S \rightarrow [D-H]^{\cdot} + [S+H]^{+}$
	$D^{+\cdot} + AB \rightarrow [D-H]^{\cdot} + [AB+H]^{+}$

Note: AB is an analyte molecule, S is a solvent molecule, and D is a dopant molecule.

Instrumentation

The pneumatic nebulizer and the heated tube are the first two components of the APPI source, and are virtually the same as those used on the APCI source. In the case of early work by Bruins and co-workers,[65] the heated nebulizer unit was taken from the original PE/SCIEX commercial APCI source.

The one component that is different from the APCI source is the photoionization lamp, consisting of a mounting bracket and a noble gas discharge lamp. This lamp can either be positioned with an orthogonal or in-line geometry. The orthogonal geometry positions the photoionization lamp perpendicular to the heated nebulizer and the sampling entrance to the mass spectrometer. Most of the laboratory built APPI sources utilize this geometry. The in-line geometry positions the photoionization lamp so that it lies along the same central axis as the entrance to the mass spectrometer. This setup places the heated nebulizer perpendicular to both the photoionization lamp and the mass spectrometer entrance and is featured on a recently developed commercial APPI source produced by Agilent Technologies. Figure 5.2 shows simple diagrams of each geometry. As of the summer of 2004, no studies had been done to compare the relative effectiveness of these geometries. The choice of a correct solvent is another important factor in APPI mass spectrometry since solvent molecules can be involved in reactions that lead to ionization of the analyte. It is important to choose a solvent that has an ionization
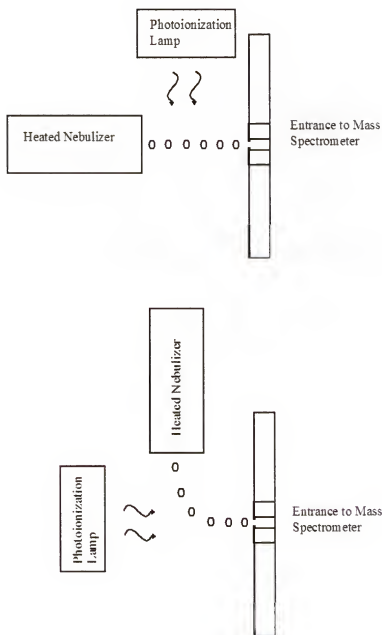
Figure 5.2 Two potential photoionization lamp geometries used in APPI.

energy above the emitted photon energies of the photoionization lamp. This minimizes

the number of interferences from the solvent because the solvent will not be

photoionized. One example of the importance of solvents can be found in the research of Yang and Henion.[78] They performed APPI mass spectrometry studies of idoxifene in different mixtures of methanol and water, and discovered that decreased water concentration led to increased sensitivity with APPI.

Estrogens and Estrogen Derivatives

Estrogens are a group of steroidal compounds that serve a variety of functions in females and males. They are produced primarily in the ovaries, and are responsible for the development and function of secondary sex organs in females.[79]

Recent research has highlighted the fact that estrogens may play a protective role in the brain. They are known to have protective properties in treatment of brain injury (strokes), neurodegredation, and cognitive degeneration based on epidemiological studies.[80] The exact reaction pathways responsible for these beneficial effects are still unknown, however evidence now exists that the estrogens may have a free-radical scavenging antioxidant effect. This may allow the estrogen compounds to act as a "chemical shield" against certain free radicals.[81,82]

Incidents such as trauma can release unbound metal ions from damaged cells.[83] These ions, such as Fe^{2+}, can result in reactions with H_2O_2 produced either spontaneously or as a result of enzyme catalyzed dismutation. The products formed by this reaction are the oxidized metal ion, hydroxide ions, and the hydroxyl radical.

$$H_2O_2 + M^{(n-1)+} \rightarrow M^{n+} + \bullet OH + \text{-}OH \ ^{13}$$

Due to the inherent reactivity of a radical species, these hydroxyl radicals can cause significant damage to the body if they are not neutralized. Recent work by Prokai *et al.*, has suggested that the phenolic hydrogen of estrogens may provide a pathway by which the hydroxyl radical can be neutralized.[84]

Current research in the Prokai group is focused on the production of various derivatives of estrogen. The reactivity and radical scavenging capabilities of these derivatives is being tested to determine their possible therapeutic effect. Unfortunately, these compounds have proven difficult to analyze via ESI or APCI. APPI was chosen as a potential new ionization technique for the mass spectrometric analysis of estrogen derivatives.

Experimental

The instrumentation used for these experiments was modified to run on a quadrupole ion trap mass spectrometer (LCQ, ThermoFinnigan, San Jose, CA). It was decided that the heated nebulizer design for the existing APCI source would be duplicated. In addition, this would minimize the amount of tuning necessary when changing between the APCI and APPI source. This would additionally serve to allow the nebulizer and sheath gas flow of the APCI source to be used with no change in parameters.

The entire setup was designed to mount to an aluminum platform that could be adjusted to allow off-axis operation if that feature was needed. The aluminum platform was also designed so that the setup could be easily converted to replace the ESI needle on the Analytica source used in Chapter 4. The heated nebulizer is mounted to the metal platform. This unit is then placed onto a mounting unit shown in figure 5.3.
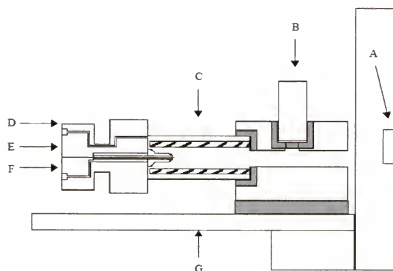
Figure 5.3. Cutaway schematic of the APPI ionization source. A is the mass spectrometer inlet. B is the photoionization lamp. C is the heated tube, the striped bars indicate the resistive heating element. D is the auxiliary gas inlet. E is the capillary inlet for sample introduction. F is the sheath gas inlet. G is the aluminum mounting platform. The gray areas represent Macor pieces used for electrical insulation.

The mounting unit was a square block that enabled the photoionization lamp to be positioned perpendicular to the path of the ions. The mounting unit was electrically insulated from the lamp, the heated nebulizer, and the metal platform. This allowed a potential to be applied to the mounting unit to further facilitate ion transport. This potential was provided by a high voltage power supply.

The photoionization lamp used in this study was a krypton discharge lamp filled with krypton. This two most intense emission lines for krypton have photon energies of 10.0 and 10.6 eV. The lamp was purchased from Cathodeon USA (Plainsville, NY).

The lamp arrived with a high voltage power supply without connections to interface to either the available house power or the ionization lamp.. The high voltage power

supply is used to initiate and maintain the krypton glow discharge inside the photoionization lamp. A circuit was designed with the assistance of the UF Chemistry electronic shop that included a method for controlling the amplitude of the high voltage as well as a power supply to convert the 110 V AC wall voltage to 10 V DC. Contacts to connect the power supply with the lamp electrodes were designed and constructed with the assistance of the UF Chemistry machine shop. This allowed rough control of the amplitude of the high voltage used to maintain the discharge in the lamp, which was sufficient since it was determined that the amplitude of the high voltage did not have a significant effect on signal.

Samples were prepared using HPLC grade solvents purchased from Sigma-Aldrich (Milwaukee, WI). Solvents were filtered by a vacuum filtration system using micron filter paper to remove particulates that might otherwise clog the capillaries.

Results

Initial attempts utilized a 500 μM solution of estrone (3-hydroxyestra-1,3,5(10)-trien-17-one, molecular weight: m/q 270) in a solution of 95%:5% acetonitrile and water. No signal was obtained until 100 μmol of a toluene dopant was added to the solution. Spectra obtained in positive ion mode were dominated by a large peak at m/q 267.3, which was attributed to $[M-3H]^+$. Running a blank caused the signal to disappear, as did modifying the ion optics to favor negative ions. The APPI source was open to the atmosphere, so there is the possibility of oxygen radicals from atmospheric oxygen reacting with hydrogens on the estrone. A 500 μM solution of estradiol (Estra-1,3,5(10)-triene-3,17beta-diol, molecular weight: m/q 272) run using the same solvent solution and

the same conditions also produced a peak that was 3 daltons lower than expected, located at m/q 269.3.

Leinonen and researchers determined that acetonitrile was one of the least sensitive solvents to use for the analysis of anabolic steroids using APPI mass spectrometry.[85] Yang and Henion determined that the inclusion of water in methanol decreased the sensitivity of APPI mass spectrometry towards idoxiphene and its metabolites.[78] Based on their conclusions, a new solvent system was chosen, composed of 100% methanol. With the new solvent system it is was possible to obtain mass spectra for estrone and estradiol. E1 quinol (10β-Hydroxyestra-1,4-dien-3,17-dione, Molecular weight: m/q 269), a laboratory synthesized estrogen derivative was also analyzed and signal was observed for the [M]$^+$ and [M+H$_2$O]$^+$ ions. An APPI spectrum of E1 quinol in a solution of 100% methanol is shown in figure 5.5.
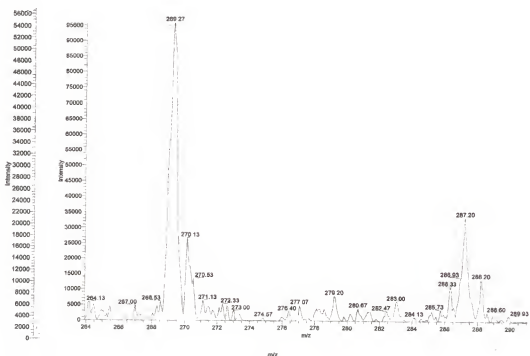
Figure 5.5. APPI mass spectrum of E1 quinol in 100% MeOH.

This spectrum can be compared to one (seen in figure 5.6) collected using APCI on the same mass spectrometer and using the same E1 quinol solution.
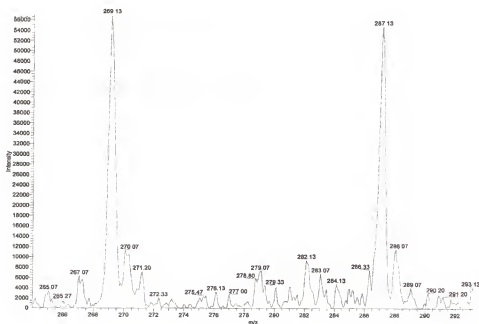
Figure 5.6. APCI mass spectrum of E1 quinol in 100% MeOH.

The ratio of the peak intensities in the APCI spectra match those obtained previously for E1 quinol in previous studies using APCI mass spectromtery.[83]

It is interesting to note that the [M]$^+$ signal is more intense in the APPI spectrum when compared to the APCI spectrum. The signal intensity for [M]$^+$ is almost twice as large as the corresponding signal intensity in the APCI spectrum. The [M+H$_2$O]$^+$ is twice as intense in the APCI spectrum as the equivalent signal in the APPI spectrum. Unfortunately, the signal to noise ratio for the APPI spectrum is not to be significantly higher than the APCI spectrum. Changes in the solvent and dopant composition should increase the APPI signal.

Conclusions

APPI is a new technique allowing for the atmospheric pressure ionization of compounds. It offers an ionization technique amenable to samples with either low proton affinities or high ionization energies. This research has shown that a laboratory-built APPI source can be combined with a commercial mass spectrometer to provide a new method for ionizing estrogens by mass spectrometry. Samples included estrone, estradiol, and E1 quinol in acetonitrile/water and methanol. Analysis of all three samples has shown the importance of the solvent for APPI analysis. The resulting data do not indicate that APPI is a far superior technique when compared to APCI for the analysis of estrogens, but they provide an alternative ionization source for further research on estrogen derivatives.

CHAPTER 6
CONCLUSIONS AND FUTURE STUDIES

The chapters in this dissertation have provided ample evidence of the power of ion preselection through rf voltage frequency adjustment in an external multipole ion guide combined with FTICR mass spectrometry. The ultrahigh mass resolution and mass accuracy of FTICR mass spectrometry are advantageous when combined with the increased sensitivity toward low abundance, high mass ions.

The glow discharge ionization source can be used in conjunction with FTICR mass spectrometry to provide a powerful tool for elemental analysis. The high mass resolving power of FTICR mass spectrometry can potentially eliminate the problem of isobaric interferences. Unfortunately, the nature of space charge effects in the the FTICR analyzer cell prevents the detection of low abundance analyte ions in the presence of high abundance background ions. While it is possible to remove undesirable background ions inside the FTICR analyzer cell, this does not increase the population of analyte ions available for detection. By selectively removing the high abundance ions in an external multipole prior to the analyzer cell, it was possible to increase the number of analyte ions in the cell.

Initial experiments focused on a copper sample analyzed with GD mass spectrometry. A mass spectrum obtained without preselection shows a strong copper signal with a large grouping of low mass background ions. By adjusting the applied rf voltage of the octopole, it was possible to cause the removal of the low mass ions. The

appearance of a previously undetectable argon dimer signal was observed in the spectrum. Based on these results, the technique of external ion preselection was expanded to a more complicated sample.

A NIST certified brass sample was analyzed using GD FTICR mass spectrometry with an external laboratory-built octopole ion guide. The primary components of brass are iron and zinc, so removal of these species along with any low mass background ions should result in increased sensitivity to the high mass low abundance species in the sample, such as Pb. A mass spectrum obtained without preselection showed a large signal for copper (61.34% abundant), zinc (35.36% abundant), and a small signal for lead (2.72% abundant). By adjusting the applied rf voltage of the octopole, it was possible to severely attenuate the copper and zinc signals while increasing the lead signal. After the frequency preselection, it was also possible to see a signal for tin (0.42% abundant) that was previously undetectable without ion preselection.

Future work in glow discharge mass spectrometry will focus on further exploring the potential of preselection by applying the technique to other samples and possibly some real world samples. Preselection is ideally suited for environmental analysis due to the fact that most environmental samples of interest have relatively high mass analytes found in low abundance.

Milgram and Eyler have proven that the inductively coupled plasma ionization source can be interfaced to the FTICR mass spectrometer to provide high mass resolving power capabilities to the analysis of environmental samples.[86] Ion preselection in an external multipole would greatly enhance the sensitivity of this technique and make ICP FTICR mass spectrometry a more attractive choice for elemental analysis.

The technique of ion preselection was then expanded to a hexapole in a commercial electrospray ionization source. A contaminated sample of Angiotensin II was analyzed using ESI on a FTICR mass spectrometer. The contamination was due to an high concentration of acetic acid as a solvent. This contamination caused a high abundance of acetate ion clusters which overwhelmed the Angiotensin II signal. A frequency generator and power amplifier were interfaced with the commercial source to provide the ability to perform ion preselection experiments. By adjusting the applied rf frequency of the hexapole, it was possible to attenuate the acetate ion cluster signal. It was possible to see the 1+ charge state of Angiotensin that was previously undetectable. A commercial tuning solution composed of a proprietary combination of compounds was then analyzed by ESI FTICR mass spectrometry. It was shown that by decreasing the frequency of the applied rf, it was possible to have the hexapole act as a variable high-pass mass filter. Future work in this area would involve expanding the technique to commercial sources other than those used on the Bruker FTICR mass spectrometer. Experiments have shown that even a small amount of attenuation of the high abundance ions can show significant improvement in the signal intensity of high mass, low abundance species.

Due to the ease by which this technique may be implemented, it is possible to expand ion preselection by frequency modulation to a large variety of ionization sources and mass analyzers. Future work would include the further characterization of the operating parameters of the hexapole ion guide. It would be useful to explore the mass resolving power of this technique to compare with that seen when using a quadrupole or octopole of the same size.

It is important to note that the stability regions of the hexapole and octopole have very poorly defined and rounded edges. Larger order multipoles will therefore have poorer mass resolving power when compared to the quadrupole used as a mass filter. If one was interested in building ion preselection into a new instrument, the well-defined quadrupole would be the obvious choice. The research presented in this dissertation will mostly likely see use on already existing instrumentation. The ESI research has already shown that ion preselection in an external multipole ion guide can be achieved simply with a commercial source.

Atmospheric pressure ionization sources have become popular tools in recent years for mass spectrometric analysis of biological samples. APPI utilizes a photoionization lamp to initiate chemical reactions in a fine mist of analyte and solvent sprayed form a heated nebulizer. By choosing solvents with ionization energies above the photon energies of the photoionization lamp it is possible to inhibit the ionization of solvent ions.

Some biological samples can prove troublesome when analyzed with APCI and ESI sources and produce erroneous signal, if any signal at all. An atmospheric pressure photoionization source was constructed for the analysis of certain laboratory synthesized estrogen derivatives. These compounds had proved troublesome to analyze in the past and it was hoped that APPI would provide greater sensitivity toward these estrogen derivatives.

Early attempts to obtain signal determined that the APPI ionization source was very dependent upon solvent conditions. While it was not conclusively shown that APPI is superior to APCI, further experimentation with solvent conditions may prove fruitful in increasing the sensitivity of APPI to estrogen derivatives. Future work would involve the exploration of a wide range of solvent systems that could enhance the sensitivity of this

technique. Signal might also be improved if the entire system is enclosed in a nitrogen purged enclosed container to prevent reactions with ambient air molecules. Finally, it would be very useful to transfer this ionization source to the FTICR mass spectrometer to allow for the ionization of an even wider variety of analytes.

REFERENCES

1. Hipple, J. A., Sommer, H., Thomas, H. A., *Phys Rev.* **1949**, 76, p. 1877.

2. Baldeschwieler, J. D., Randall, E. W., *Acc. Chem. Res.* **1963**, 63, p. 81.

3. McIver, R. T., Jr., *Rev. Sci. Instrum.* **1970**, 41, p. 555.

4. Marshall, A. G., *Acc. Chem. Res.* **1985**, 18, p. 316.

5. Comisarow, M. B., Marshall, A.G., *Chem. Phys. Lett.* **1974**, 4, p. 284.

6. Marshall, A. G., Hendrickson, C. L., Jackson, G. S., *Mass Spec. Rev.* **1998**, 17:1, p. 1.

7. Limbach, P. A., Grosshans, P. B., Marshall, A. G., *Anal. Chem.* **1993a**, 65, p. 135.

8. Makarov, A., *Anal. Chem.* **2000**, 72, p. 1156.

9. Guan, S. H., Marshall, A. G., *Int. J. Mass Spectrom. Ion Process.*, **1996**, 158, p. 5.

10. Shi, S. D. H., Drader, J. J., Hendrickson, C. L., Marshall, A.G., *J. Am. Soc. Mass. Spectrom.* **1999**, 10, p. 265.

11. Marshall, A. G., Schweikhard, L., *Int. J. Mass Spectrom.* **1990**, 101, p. 37.

12. Hettich, R. L., Buchanan, M .V., *Int. J. Mass Spectrom. Ion Proc.* **1991**, 111, p. 365.

13. Lebrilla, C. B., Wang, D. T. -S., Hunter, R. L., McIver, R. T. Jr., *Anal. Chem.* **1990**, 62, p. 878.

14. Kofel, P., Alleman, M., Kellerhals, H., Wancek, K., *Int. J. Mass Spectrom. Ion Proc.*, **1985**, 65, p. 97.

15. McIver, R. T. Jr., Hunter, R. L., Bowers, W. D., *Int. J. Mass Spectrom. Ion Proc.* **1985**, 64, p. 67.

16. Huan, Y. L., Guan, S., Kim, H. S., Marshall, A. G., *Int. J. Mass Spectrom. Ion Proc.* **1996**, 152, p. 121.

17. Thomson, J. J., *Philos. Mag.*, **1897**, 44, p. 293.

18. Denison, D. R., *J of Vac. Sci. Tech.*, **1971**, 8:1, p. 266.

19. Miller, P. E., Denton, B. M., *J. of Chem. Ed.* **1986**, 63:7, p. 617.

20. Mathieu, E., *J. de Math. Pure et App.* **1860**, 5, p. 9.

21. Mathieu, E., *J. de Math. Pure et App.* **1861**, 6, p. 241.

22. Mathieu, E., *J. de Math. Pure et App.* **1873**, 18, p. 25.

23. Hagg C., Szabo I., *Int. J. Mass Spectrom. Ion Process.* **1986**, 73, p. 277.

24. Gerlich, D., *State Selected And State-To-State Ion-Molecule Reaction Dynamics* Eds. N. B. Cheuk-Yiu, M., John Wiley & Sons, Inc., New York, **1992**, Chapter 1.

25. Guzowski, J. P., Jr., Hieftje, G. M., *J. Anal. Atom. Spectrom.* **2001**, 16:6, p. 781.

26. Tanner, S. D. and Baranov, V. I., *Atom. Spectros.* **1999**, 20:2, p. 45

27. Wang, Y., Shi, S. D. H., Hendrickson, C. L., Marshall A. G., *Int. J. Mass Spectrom.* **2000**, 198, p. 113.

28. Paul, W., Raether, M., *Zeit. fur Phys.* **1955**, 140, p. 262.

29. Marmet, P., Proulx, M., *Int. J. Mass Spectrom. Ion Process.* **1982**, 42, p. 3.

30. Voyksner, R. D., Lee, H., *Rapid Commun. Mass Spectrom.*, **1999**, 13, p. 1427.

31. Duckworth, D. C., Eyler, J. R., Watson, C. H. *Inorganic Mass Spectrometry: Fundamentals and Applications* Eds. Barshick C.M., Duckworth, D.C., Smith, D.H., Marcel Dekker, New York, **2000**; Chapter 9.

32. Thomson, J. J., *Rays of Positive Electricity and their Application to Chemical Analysis*, Longmans, Green, New York, **1913**.

33. Aston, F., *Mass Spectra and Isotopes*, Arnold, London, **1942**.

34. Dempster, A. J., *Phys. Rev.* **1937**, 51, p. 67.

35. Marcus, R. K., Broekaert, *Glow Discharge Plasmas in Analytical Spectroscopy*, J. A. C. Ed., Wiley, New York, 2003.

36. Wagatsuma, K., *Spectrochm. Acta, Part B* **2001**, 56, p. 465.

37. Coburn, J. W., Harrison, W. W., *Appl. Spectrosc. Rev.* **1981**, 17, p. 95.

38. Tanner, S. D., *J. Anal. Atom. Spectrom.* **1995**, 10, p. 905.

39. Deng, R. C., Williams, P., *Anal. Chem.* **1994**, 66, p. 1890.

40. Su, Y. X., Yang, P. Y., Zhou, Z., Li, F. M., Wang, X. R., Huang, B. L., *J. Anal. Atom. Spectrom.* **1998**, 13, p. 1271.

41. Smith, F. G., Wiederin, D. R., Houk, R. S., *Anal. Chem.*, **1991**, 63, p. 1458.

42. Eiden, G. C., Barinaga, C. J., Koppenaal, D. W., *J. Anal. Atom. Spectrom.* **1996**, 11, p. 317.

43. Du, Z. Y., Houk, R. S., *J. Anal. Atom. Spectrom.* **2000**, 15, p. 383.

44. King, F. L., Harrison, W. W., *Mass Spectrom. Rev.*, **1990**, 9, p. 285.

45. Eiden, G. C., Barinaga, C. J., Koppenaal, D. W., *J. Anal. Atom. Spectrom.* **1999**, 14, p. 1129.

46. Shohet, J. L., Phillips, W. L., Lefkow, A. R. T., Taylor, J. W., Bonham, C., Brenna, J. T., *Plasma Chem. and Plasma Proc.*, **1989**, 9, p. 207.

47. Marcus, R. K.; Cable, P. R.; Duckworth, D. C.; Buchanan, M.V.; Pochkowski, J.M.; Weller, R. R., *Appl. Spectrosc.* **1992**, 46, p. 1327.

48. Barshick, C. M., Eyler, J. R., *J. Amer. Soc. Mass Spectrom*, 1993, **4**, p. 387.

49. Watson, C. H., Wronka, J., Laukien, F. H., Barshick, C. M., Eyler, J. R., *Spectrochim. Acta, Part B*, **1993**, 48, p. 1445.

50. de Koning, L. J., Nibbering, N. M. M., van Orden, S. L., Laukien, F. H. *Int. J. Mass Spectrom. Ion Process.*, **1997**, 165, p. 209.

51. Senko, M. W., Canterbury, J. D. , Guan, S. H. Marshall, A. G., *Rapid Comm. Mass Spectrom.* **1996**, 10, p. 1839.

52. Blakney, G. T., van der Rest, G., Johnson, J. R., Freitas, M. A., Drader, J. J., Shi, S. D.-H., Hendrickson, C. L., Kelleher, N. L., Marshall, A. G., *Further Improvements to the MIDAS Data Station for FT-ICR Mass Spectrometry*, 49th Amer. Soc. Mass Spectrom. Conf. on Mass Spectrom. & Allied Topics, Chicago, IL, May, **2001**.

53. Hastings, E. P., Harrison, W. W., *J. Anal. Atom. Spectrom.*, **2004**, 19, p. 1268.

54. Rayleigh, L. L., *Philosph. Mag.* **1882**, 14, p. 184.

55. Cody, R. B., Burnier, R. C., Freiser, B. S. *Anal. Chem.* **1982**, 54, p. 96

56. Woodlin, R. L., Bomse, D. S., Beauchamp, J. L., *Anal. Amer. Chem. Soc.* **1978**, 100, p. 3248.

57. Senko, M. W., Canterbury, J. D., Guan, S. H., Marshall, A. G. *Rapid Comm. Mass Spectrom.* **1996**, 10, p. 1839.

58. Wigger, M., Nawrocki, J. P., Watson, C. H., Eyler, J. R., Benner, S. A., *Rapid Comm. Mass Spectrom.* **1997**, 11, p. 1749.

59. Siegel, M. M., Tabei, K., Bebernitz, G. A., Baum, E. Z., *J. of Mass Spec.* **1998**, 33, p. 264.

60. Horning, E. C., Horning, M. G., Carroll, D. I., Dzidic, I., Stilwell, R. N. *Anal. Chem.* **1973**, 45, p. 936.

61. Horning, E. C., Carroll, D. I., Dzidic, I., Haegele, K.D., Horning, M. G., Stilwell, R. N., *J. Chromatograph. Soc.* **1974**, 12, p. 725.

62. Carroll, D. I., Dzidic, I., Stilwell, R. N., Haegele, K.D., Horning, E. C. *Anal. Chem.*, **1975**, 47, p. 2369.

63. Sunner, J.; Nicol, G.; Kebarle, P. *Anal. Chem.* **1988**, 60, p. 1300.

64. Sunner, J.; Ikonomou, M.G.; Kebarle, P. *Anal. Chem.* **1988**, 60, p. 1308.

65. Carroll, D. I.; Dzidic, I.; Horning, E. C.; Stillwell, R. N. *App. Spectros. Rev.* **1981**, 17, p. 337.

66. Robb, D.B., Covey, T.R., Bruins, A. P., *Anal Chem,* **2000**, 72, p. 3653.

67. Trickl, T., Cromwell, E. F., Lee, Y. T., Kung, A. H. *J. Chem. Phys.* **1989**, 91, p. 6006.

68. Ruett, J. E., Wang, L, S., Lee, Y. T., Shirley, D.A. *J. Chem. Phys.*, **1986**, 85, p. 6928.

69. Gochel-Dupuis, M., Delwiche, J., Hubin-Franskin, M.-J., Collin, J.E., *Chem. Phys. Lett.* **1992**, 193, p. 41.

70. Tokyn, R. G., Winniczek, J. W., White, M. G. *Chem. Phys. Lett.* **1989**, 164, p. 137.

71. Holmes, J. L., Lossing, F. P. *Org. Mass Spectrom.* **1991**, 26, p. 537.

72. Bowen, R. D., Maccoll, A. *Org. Mass Spectrom.* **1984**, 19, p. 379.

73. Lias, S. G., *Ion Cyclotron Reson. Spectrom.* **1982**, 1982, p. 409.

74. Traeger, J. C., McLoughlin, R. G., Nicholson, A. J. C., *J. Am. Chem. Soc.* **1982**, 104,
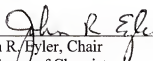
p. 5318.

75. Lifshitz, C., *J. Phys. Chem.* **1982**, 86, p. 606.

76. Nemeth, G. I., Selzle, H. L., Schlag, E.W., *Chem. Phys. Lett.* **1993**, 215, p. 151.

77. Lu, K.-T., Eiden, G. C., Weissharr, J. C., *J. Phys. Chem.* **1992**, 96, p. 9742.

78. Yang, C., Henion, J. *J. Chromatograph. A* **2002**, 970, p. 155.

79. Lubay, G., *Biochemistry*, 4th Ed.; WMC Brown Publishing, **1996**, p. 675

80. Vedder, H., Anthes, N., Stumm, G., Wurz, C., Behl, C., Krieg, J. C., *J. Neurochem.* **1999**, 72, **p.** 2531.

81. Halliwell, B., *Drugs Aging* **2001**, 18, p. 685.

82. Bishop, G. M., Robinson, S. R. *Brain Res.* **2001**, 90, p. 175.

83. Halliwell, B., *J. Neurochem.* **1992**, 56, p. 1609.

84. Prokai, L., Prokai-Tatrai, K., Perjesi, P., Zharikova, A.D., Perez, E.J., Liu, R., Simpkins, J.W., *Proc. Natl. Acad. Sci.*, **2003**, 100:20, p. 11741.

85. Leinonen, A., Kuuranne, T., Kostiainen, R., *J. Mass Spectrom.* **2002**, 37, p. 693.

86. Milgram, K. E., White, F. M., Goodner, K. L., Watson, C. H., Koppenaal, D. W., Barinaga, C. J., Smith, B. H., Winefordner, J. D., Marshall, A. G., Houk, R. S., Eyler, J. R., *Anal. Chem.* **1997**, 69, p. 3714.

BIOGRAPHICAL SKETCH

Keith David Zientek was born in Palm Beach Gardens, FL, on December 30th, 1976. He is the first child of Helen and Chester Zientek. Keith spent most of his younger years in constant movement, living in places such as Hartford, Las Vegas, San Antonio, Fort Walton Beach, Saudi Arabia, and Egypt with his parents and his sole sibling, Emily Zientek. His parents eventually settled back in Palm Beach Gardens in 1988. He attended the Palm Beach County School of the Arts for 5 years and specialized in theatre.
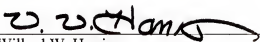
Keith graduated from Richmond College at the University of Richmond with a Bachelor of Science in chemistry. While at Richmond, Keith performed research under Dr. Samuel Abrash in computational chemistry on the excited states of the methyl methoxy radical. Keith was a captain of the men's diving team his senior year and held a school record for the 1-meter springboard. After graduating from Richmond, Keith decided to pursue graduate studies in analytical chemistry at the University of Florida under the direction of John R. Eyler.

I certify that I have read this study and that in my opinion it conforms to acceptable standards of scholarly presentation and is fully adequate, in scope and quality, as a dissertation for the degree of Doctor of Philosophy.

John R. Eyler, Chair
Professor of Chemistry

I certify that I have read this study and that in my opinion it conforms to acceptable standards of scholarly presentation and is fully adequate, in scope and quality, as a dissertation for the degree of Doctor of Philosophy.
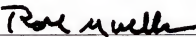
Willard W. Harrison
Professor of Chemistry

I certify that I have read this study and that in my opinion it conforms to acceptable standards of scholarly presentation and is fully adequate, in scope and quality, as a dissertation for the degree of Doctor of Philosophy.
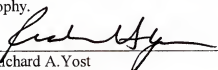
David H. Powell
Scientist of Chemistry

I certify that I have read this study and that in my opinion it conforms to acceptable standards of scholarly presentation and is fully adequate, in scope and quality, as a dissertation for the degree of Doctor of Philosophy.

Paul A. Mueller
Professor of Geological Sciences

I certify that I have read this study and that in my opinion it conforms to acceptable standards of scholarly presentation and is fully adequate, in scope and quality, as a dissertation for the degree of Doctor of Philosophy.

Richard A. Yost
Professor of Chemistry

This dissertation was submitted to the Graduate Faculty of the College of Liberal Arts and Sciences and to the Graduate School and was accepted as partial fulfillment of the requirements for the degree of Doctor of Philosophy.

December 2004

_____

Dean, Graduate School